

Spring 2018

# Designing and Testing 3-D Printed Wafer-box with Embedded PZT Sensors to Identify the Shape Effect on Energy Harvesting

Ahmad Jami Safayet

Follow this and additional works at: <https://digitalcommons.georgiasouthern.edu/etd>



Part of the [Civil Engineering Commons](#), [Construction Engineering and Management Commons](#), [Electrical and Electronics Commons](#), [Electronic Devices and Semiconductor Manufacturing Commons](#), [Energy Systems Commons](#), [Other Civil and Environmental Engineering Commons](#), [Other Electrical and Computer Engineering Commons](#), [Other Mechanical Engineering Commons](#), [Power and Energy Commons](#), [Structural Engineering Commons](#), and the [Transportation Engineering Commons](#)

---

## Recommended Citation

Safayet, Ahmad Jami, "Designing and Testing 3-D Printed Wafer-box with Embedded PZT Sensors to Identify the Shape Effect on Energy Harvesting" (2018). *Electronic Theses and Dissertations*. 1751.

<https://digitalcommons.georgiasouthern.edu/etd/1751>

This thesis (open access) is brought to you for free and open access by the Graduate Studies, Jack N. Averitt College of at Digital Commons@Georgia Southern. It has been accepted for inclusion in Electronic Theses and Dissertations by an authorized administrator of Digital Commons@Georgia Southern. For more information, please contact [digitalcommons@georgiasouthern.edu](mailto:digitalcommons@georgiasouthern.edu).

# DESIGNING AND TESTING 3-D PRINTED WAFER-BOX WITH EMBEDDED PZT SENSORS TO IDENTIFY THE SHAPE EFFECT ON ENERGY HARVESTING

by

AHMAD JAMI SAFAYET

(Under the Direction of Seonghoon Kim)

## ABSTRACT

Piezoelectric energy has been recently paid attention in the field of alternative energy. Day by day the traditional energy sources including Coal tar and oils are becoming scarce. People are heading to an alternative energy source to meet the future energy demand. Piezoelectric energy is one of the competitive energy sources compared to the conventional renewable energy sources including solar, wind, and geothermal power and so on. This energy production method bears enormous research potential because it can be used as the roadway for a new method of power generation. This research project aimed to identify which shaped wafer-box produced the higher electricity. This research project utilized both a 3-D printer and a 3-D Computer Aided Design (CAD) to develop five different shapes of prototype wafer boxes coupled with piezoelectric sensors. Various forms were developed see if there were any potential difference in power (voltage) generation due to the structure of the box. In order to run an Asphalt Pavement Analyzer (APA) wheel load test, piezoelectric ceramic disk sensor was embedded into the wafer box. Collected data from the APA load wheel test were analyzed using various statistical methods which produced significant findings. The analytical result indicated that out of the five different shaped wafer boxes the circularly shaped box produced the highest average voltage values. The triangular shape is in the second position to produce voltage. The square shape is in the lowest position of the list to produce electricity. The 3-D printers can print wafer-box with other different materials for testing. The 3-D printer can print the product accurately which gives the more reliable output. These 3-D printed wafer-boxes could be can be utilized for APA testing to determine the effectiveness. Additional research could lead to a broader understanding of PZT-based energy harvesting technology as well as providing a platform for testing PZT harvest units.

INDEX WORDS: Piezoelectricity, PZT Materials, Sensors, Voltage, Wafer-box, Experiment design, Section modules

DESIGNING AND TESTING 3-D PRINTED WAFER-BOX WITH  
EMBEDDED PZT SENSORS TO IDENTIFY THE SHAPE EFFECT ON  
ENERGY HARVESTING

by

AHMAD JAMI SAFAYET

(Under the Direction of Seonghoon Kim)

B.S., Bangladesh University of Engineering and Technology, Bangladesh, 2014

MS, Georgia Southern University, 2018

A Thesis Submitted to the Graduate Faculty of Georgia Southern University in  
Partial Fulfillment of the Requirements for the Degree

MASTER OF SCIENCE

STATESBORO, GEORGIA

© 2018

AHMAD JAMI SAFAYET

All Rights Reserved

DESIGNING AND TESTING 3-D PRINTED WAFER-BOX WITH  
EMBEDDED PZT SENSORS TO IDENTIFY THE SHAPE EFFECT ON  
ENERGY HARVESTING

by

AHMAD JAMI SAFAYET

Major Professor: Seonghoon Kim

Committee: Junan Shen

Mohammad Ahad

Electronic Version Approved:

May 2018

## DEDICATION

To my beloved family: My parents, my wife, my brother and sister.

## ACKNOWLEDGMENT

First, I would like to express my earnest gratefulness to my advisor, Professor Dr. Seonghoon Kim, Associate Professor, Department of Civil Engineering and Construction Management at Georgia Southern University. His continuous support of my Masters program of study and related research was evidenced by his patience, active encouragement, thoughtful suggestions and sharing of his vast knowledge. Dr. Seonghoon Kim provided invaluable guidance throughout my Masters program and his mentorship created an unparalleled graduate education.

Second, I would like to thank the rest of my thesis committee: Professor Dr. Junan Shen, and Professor Dr. Mohammad Ahad, for their insightful comments and encouragement which provided the incentive for me to widen my research to include various perspectives.

Third, I would like to thank my family: my parents and to my brothers and sister and my spouse for supporting me profoundly throughout writing this thesis and my life in general.

## TABLE OF CONTENTS

ACKNOWLEDGMENTS .....	3
LIST OF TABLES .....	7
LIST OF FIGURES .....	8
CHAPTER .....	11
1 INTRODUCTION .....	11
1.1 Background.....	11
1.2 Problem statement .....	12
2 OBJECTIVES OF RESEARCH, SCOPE AND RESEARCH FRAMEWORK	13
2.1 Research objectives .....	13
2.2 Scope of the research .....	13
2.3 Research framework .....	16
3 LITERATURE REVIEW.....	18
3.1 ASTM Standards .....	18
3.1.1 Standard test method for flexural strength of concrete (using simple beam with third-point loading).....	20
3.1.2 Standard test method for obtaining and testing drilled cores and sawed beams of concrete .....	20
3.1.3 Splitting tensile strength of cylindrical concrete specimens (ASTM C- 496).....	21
3.1.4 Mounting piezoelectric emission sensors.....	22
3.1.5 Standard test method for tensile properties of plastics (ASTM D 638 - 02a) .....	22



3.2 UL Global standard.....	23
3.2.1 Standard for supplementary protectors for use in electrical equipment	24
3.2.2 Safety Requirements for electrical equipment for measurement, control, and laboratory use.....	24
3.3 Case study of energy harvesting using PZT sensors .....	26
3.4 Factors affecting piezoelectric energy harvesting .....	27
3.4.1 Thickness-Area ratio .....	28
3.4.2 Shape Effect of Piezoelectric Energy Harvester on Vibration Power Generation (Case study 1) .....	28
3.4.3 Shape Effect of Piezoelectric Energy Harvester (Case study 2) .....	30
3.4.4 Temperature effect on piezoelectric energy harvesting .....	30
3.5 Experimental research design.....	31
3.5.1 True experimental design .....	31
3.6 Summary of Literature Review .....	33
3.7 Controversies of some research papers .....	34
4 METHODOLOGIES .....	35
4.1 Equipment for testing .....	35
4.1.1 Asphalt Pavement Analyzer-Junior (APA Jr.) .....	36
4.1.2 Oscilloscope.....	38
4.1.3 3D-Printer .....	39
4.1.4 Circular Ceramic disc sensor.....	39
4.2 Wafer box design in CAD .....	41
4.3 3D-Printer for printing model wafer-box .....	45
4.3.1 Printer hosts .....	45
4.3.2 Printing 3D Model.....	45
4.4 Embedding PZT sensor in wafer-box.....	48
4.5 Designing circuits for recalculation of generating power and energy .....	49

4.6 Experimental design for data collection .....	52
4.6.1 Preliminary experimental design.....	52
4.6.2 Final experimental design for final data collection .....	53
4.7 Statistical methods used for data analysis .....	57
4.7.1 One-way ANOVA analysis .....	58
4.7.2 Tukey HSD test .....	60
4.7.3 Scheffe's method.....	60
5 RESULTS AND DISCUSSION .....	62
5.1 Data analysis .....	62
5.1.1 Results of preliminary experimental design.....	62
5.1.2 Result of final experimental design.....	63
5.2 Statistical analysis of voltage data generated by twenty-five PZT sensors.....	65
5.2.1 One-way ANOVA analysis .....	65
5.2.2 Results of Tukey HSD Test.....	67
5.2.3 Results of Scheffe's method .....	68
6 CONCLUSIONS AND RECOMMENDATIONS .....	70
REFERENCES.....	73
APPENDIX A.....	77
APPENDIX B .....	95
APPENDIX C .....	96
APPENDIX D.....	106

## LIST OF TABLES

Table 1: APA (Asphalt Pavement Analyzer) Jr. machine specification .....	37
Table 2: Possible Combinations of PZT sensors and Wafer-box .....	53
Table 3: Five blocks of PZT sensors.....	53
Table 4: Possible combinations of five different shaped Wafer box and twenty-five PZT sensors .....	57
Table 5: Voltage (RMS volts) produced by different wafer box coupling with PZT sensors .....	62
Table 6: Voltage (RMS volts) data generated by twenty-five PZT sensors embedded in different shaped Wafer-box under 152lbs. wheel load.....	64
Table 7: Descriptive statistics for 5 class (5 shapes) independent treatments .....	65
Table 8: Results of Tukey HSD Test for voltage data produced by twenty-five PZT sensors.....	67
Table 9: Results of Scheffe's method Test for voltage data produced by PZT sensor 1 .....	68
Table 10: Section modulus calculation equations for circular shape (Engineers Edge, 2018).....	77
Table 11: Section modulus calculation equations for triangular shape (Engineers Edge, 2018) .	78
Table 12: Section modulus calculation equations for hexagonal shape (Engineers Edge, 2018).	78
Table 13: Section modulus calculation equations for rectangular shape (Engineers Edge, 2018)	79
Table 14: Section modulus calculation equations for square shape (Engineers Edge, 2018).....	80
Table 15: Section modulus calculation for five different shapes.....	80
Table 16: Section modulus and average voltage value table .....	81
Table 17: Linear fit-curve calculation.....	81
Table 18:: Area moment of inertia and average voltage value table .....	83
Table 19: Radius of gyration and average voltage value table .....	84
Table 20: Extreme points and average voltage value table.....	85
Table 21: Summary of regression calculation with structural properties and average voltage data .....	86
Table 22: Summary of regression calculation with structural properties and 125 voltage data ...	90
Table 23: 125 voltage data and structural property value table .....	90
Table 24: Data file for PZT sensor 22 embedded in circular shaped box.....	96

## LIST OF FIGURES

Figure 1: Research Framework.....	15
Figure 2: ASTM International (ASTM International, 2018) .....	18
Figure 3: Diagrammatic view of a suitable apparatus for flexure test of concrete by third-point loading method (ASTM C 78 , 2002) .....	20
Figure 4: Suitable capping device for splitting tensile strength test (ASTM C 42/C 42M – 03, 2003) .....	21
Figure 5: A Loaded Wheel Test (LWT) (Kim et al., 2018).....	26
Figure 6: Sensors embedded in asphalt and concrete (Kim et al., 2018).....	27
Figure 7: Experimental setup and PZT devices (Basari et al., 2014) .....	28
Figure 8: Experimental setup for energy measurement (Basari et al., 2014). .....	29
Figure 9: Triangular plate size specification (Basari et al., 2014) .....	29
Figure 10: Power generator circuit (Kaur et al., 2016).....	30
Figure 11: Lab arrangement (From Left 1. APA machine, 2. 3D-printer 3. Oscilloscope, 4. Lab computer, 5. APA control computer).....	35
Figure 12: Asphalt Pavement Analyzer-APA Jr.....	36
Figure 13: Advanced Pavement Analyzer inside arrangement (APA) Jr. ....	37
Figure 14: Yokogawa DL850V scope-corder(Oscilloscope) .....	38
Figure 15: Output display of the oscilloscope .....	38
Figure 16: TAZ LULZBOT 6 3-D Printer.....	39
Figure 17: Piezoelectric sensor used to harvest energy (Top view) .....	40
Figure 18: Piezoelectric sensor used to harvest energy (Bottom view).....	40
Figure 19: Copper ribbon used with the sensors in the wafer box.....	41
Figure 20: Ceramic disc sensor attached to wafer box with two ports (Positive and negative) ...	41
Figure 21: Upper part of the wafer box (Auto CAD 2D plan view).....	42
Figure 22: Lower part of the rectangular wafer box (Auto CAD 2D plan view) .....	42
Figure 23: Hollow channel in the upper section (Top view) .....	43
Figure 24: Hollow channel in the upper part (3D wire-view) .....	43
Figure 25: Bolt dimensions.....	43
Figure 26: Isometric view of rectangular box sensor (Bottom plate) .....	44
Figure 27: Isometric view of rectangular box sensor (Top Plate) .....	44

Figure 28: A Realistic 3D model of wafer box (Top Plate).....	44
Figure 29: A Realistic 3D model of wafer box (Bottom plate) .....	44
Figure 30: File preview in the CURA 21.04 software .....	45
Figure 31: Printer host CURA 21.04 software.....	46
Figure 32: Printing wafer box with 3D printer .....	46
Figure 33: 3D-Printing material (ABS 3mm PLA).....	47
Figure 34: Hexagonal shaped wafer box .....	47
Figure 35: Triangular shaped wafer box.....	47
Figure 36: Circular shaped wafer box.....	48
Figure 37: Square shaped wafer box.....	48
Figure 38: Rectangular shaped wafer box .....	48
Figure 39: Embedded PZT sensor in wafer-box .....	49
Figure 40: A layout of the Full-wave bridge rectifier.....	49
Figure 41: Full Bridge Rectifier input and output voltage curves .....	49
Figure 42: The rectifier circuit.....	50
Figure 43: Equipment Set-up for Testing Rectified Voltages in load .....	50
Figure 44: Voltage measurement by the oscilloscope .....	51
Figure 45: Sine wave-AC current (RAE, 2018).....	51
Figure 46: Non-sinusoidal curve (Macromatic Inc, 2018).....	52
Figure 47: PZT sensors (block 1).....	54
Figure 48: PZT sensors (block 2).....	54
Figure 49: PZT sensors (block 3).....	54
Figure 50: PZT sensors (block 4).....	54
Figure 51: PZT sensors (block 5).....	54
Figure 52: Preliminary experimental design (Sensor- wafer box combination).....	55
Figure 53: Final experimental design (Sensor- wafer box combination) .....	56
Figure 54: Average voltage generated by different shaped wafer box .....	63
Figure 55: Voltage generated by PZT sensors for different shaped wafer box .....	63
Figure 56: Average voltage (RMS volts) produced by twenty-five sensors embedded with different shaped wafer box.....	68
Figure 57: Circular shape.....	77

Figure 58: Triangular shape .....	78
Figure 59: Hexagonal shape.....	78
Figure 60: Rectangular shape.....	79
Figure 61: Square shape.....	79
Figure 62: Linear regression fit-curve for section modulus and average voltage value.....	82
Figure 63:Linear regression fit-curve for area moment of inertia and average voltage value.....	83
Figure 64: Linear regression fit-curve for radius of gyration and average voltage value.....	84
Figure 65: Linear regression fit-curve for extreme points and average voltage value .....	85
Figure 66: Linear regression fit-curve for area moment of inertia and 125 voltage value .....	87
Figure 67: Linear regression fit-curve for section modulus and 125 voltage value .....	88
Figure 68: Linear regression fit-curve for radius of gyration and 125 voltage value .....	88
Figure 69: Linear regression fit-curve for extreme points and 125 voltage value.....	89
Figure 70: Output display for PZT sensor no 22 embedded in circular shaped wafer box .....	96
Figure 71: Control interface of APA-Jr software. ....	105

## CHAPTER

### 1 INTRODUCTION

#### 1.1 Background

The term “Piezoelectricity” refers to the change of the electric polarization with stress; this change results in a change in voltage across the material in the direction of the polarization (Sihai Wen, 2002). The use of the structural elements for piezoelectricity eliminates or reduces the need for embedded or attached devices, which are expensive and limited in durability, in addition to causing mechanical property degradation of the structure in the case of embedded devices.

Piezoelectricity allows the conversion of mechanical energy to electrical energy. The energy conversion can be used for the generation of electrical power. Piezoelectricity is related to the dielectric behavior. This dielectric constant is a material property that is related to the dipole electric moment per volume unit. This dipole moment is also called the polarization. Electric dipoles are present due to the presence of ionic bonding and moisture in cement. (Ang Hu, 1999).

PZT materials are currently being considered (or used) in the development of wafer boxes as well as embedded in roadways for energy. Piezoelectric materials have high energy conversion ability from mechanical vibration (Kim et al., 2011). The amount of electricity generated by piezoelectric material is comparatively low than other alternative sources. And the economic advantage of producing energy using piezoelectric materials is not very high. It is necessary to conduct more research on PZT materials to harvest energy from it in large scale.

A numerous number of researches have been conducted to develop simple and efficient energy harvesting devices from vibration by using piezoelectric materials. The researchers are trying to use the pavement as source of energy where force comes along the vertical direction. Piezoelectric energy harvesting has attracted wide attention from researchers especially in the last decade due to its high-power density, architectural simplicity, and scalability. The number of studies on piezoelectric energy have been doubled in last five years than its electromagnetic and electrostatic counterparts (Alperen Topra, 2014).

The sources of the force are vertical loads from vehicles or human. Wafer-box development is an important step to harvest energy from PZT materials. PZT sensors could be embedded into wafer-box since they do not need to be put outside like other alternative energy. Wafer-boxes could be placed in the pavement where sensors are protected from any kind of damage.

For harvesting energy, it is necessary to conduct material testing. But there is no specific standard for material testing in this subject area. ASTM and UL standards are two companies who provides the guidelines for different material testing and environmental standards. These standards could be followed to conduct material testing.

## **1.2 Problem statement**

Piezoelectricity allows the conversion of mechanical energy to electrical energy. The energy conversion can be used for the generation of electrical power. For a sustainable production of electricity, the durability of PZT materials is essential. Different climatic (temperature, pressure, salt environment) conditions could affect the production of electricity. One way of addressing the dilemma of climatic conditions could be the use of wafer boxes embedded with PZT sensors.

Ceramic disc PZT sensors were embedded into the wafer box. The wafer boxes were tested for load wheel test (LWT) in APA (Asphalt Pavement Analyzer) machine to harvest energy (voltage). It was identified, if there any shape effect on energy harvesting exists and if exist which shape produces the highest energy comparing to others. Energy generated with PZT materials was measured in the lab before the system design based on ASTM and UL standards. At the end of the research, research result could be developed and become a platform for testing Piezo-energy harvest units based on ASTM and UL standards.



## CHAPTER

### 2 OBJECTIVES OF RESEARCH, SCOPE AND RESEARCH FRAMEWORK

This chapter focuses on the objectives to be accomplished to achieve the research goal. In the next section provides brief idea about scope of the research project. The research framework is discussed in detail at the end of this chapter.

#### **2.1 Research objectives**

The prime goal of this research work was to develop ideal PZT wafer box using 3D-printer. More specifically the existence of a wafer box shape effect on energy (voltage) harvesting was examined. To accomplish this guiding research goal, it is necessary to achieve specific objectives. The objectives of this research project were:

1. Developed five different shaped prototype wafer box using the 3-D printer. This box was coupled with PZT sensors.
2. Designed experiments for conducting load wheel testing with PZT sensors embedded in wafer box.
3. Conducted Load Wheel Test (LWT) in Asphalt Pavement Analyzer (APA) machine.
4. Identified which shape produces the highest-level energy.

The advanced application of project knowledge depended on the success of the project. The accuracy of the outcome influenced the reliability of the knowledge base. The extracted knowledge from this research should be used in the future to work in broad scale and expand the workspace in this area.

#### **2.2 Scope of the research**

Due to the lack of content specific standards, the ASTM and UL standards were selected as supporting guidelines by conducting a literature review. Structural properties are to be tested based on ASTM Certification. These tests are to be done using APA (Asphalt Pavement Analyzer). The scope of this research project made it possible to examine the use of plastic

materials and ceramic disk PZT electronic sensors in the design and 3-D printing of wafer-boxes. PLA (Polylactic Acid) plastic filaments were used to print wafer-box utilizing 3D-printers.

Two experiments were designed for data collection. In the preliminary experiment five sensors were used with five prototype wafer-boxes. The PZT sensor was selected following a randomization process ensuring-every PZT sensor had an equal chance of being assigned for an experiment on a random basis. In the final experiment design twenty-five PZT sensors were used. Increasing the number of PZT sensors to 25 produced five times the amount of data collected during the preliminary experiment. The increased data maintained the statistical soundness of the research.

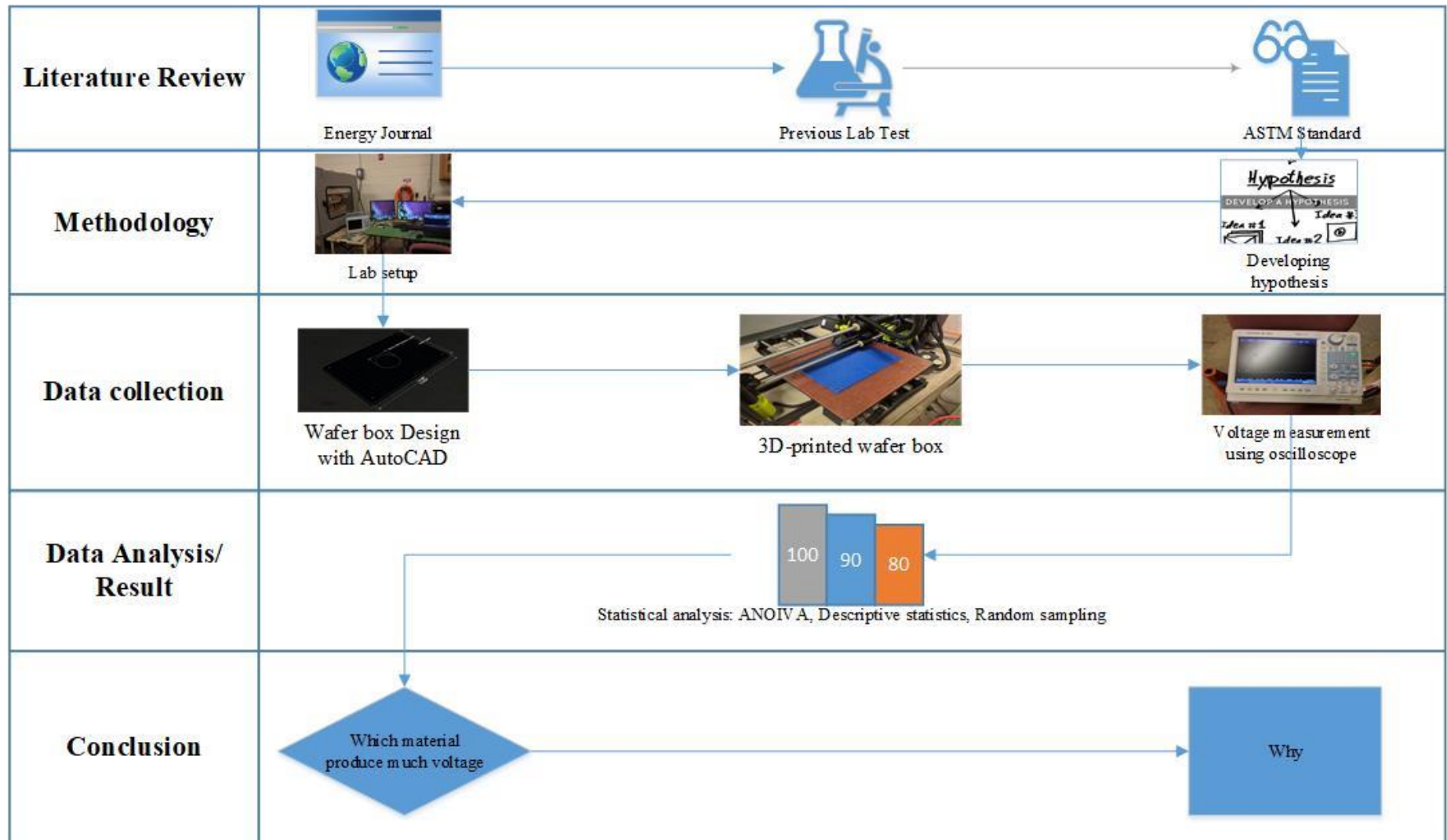


Figure 1: Research Framework

## **2.3 Research framework**

For conducting successful research, it was necessary to complete the research tasks following a detailed framework. The research team conducted the research project following the research framework described below.

### **Literature review**

A literature review was conducted to provide an analytical overview of the significance of the research topic in the area of alternative energy use in road construction. If the reader of research paper knows less than the subject, the purpose of literature review should be instructional. On the other hand, if the reader knows more than the topic, it is essential to demonstrate familiarity, expertise, and intelligence with the issue.

### **Lab setup**

Proper arrangement of equipment for testing is required for performing successful lab tests. The research was completed using equipment APA machine, oscilloscope, 3-D printer, and computer.

### **Development of the hypothesis**

Hypothesis development was a vital part of this research work since it defined exact outcome of the research. A hypothesis is an idea which suggests a possible explanation for a situation, but which has not yet been proved to be correct. To describe the rationale, two types of hypothesis were generated. One was null hypothesis and the second was an alternative hypothesis.

### **Design of wafer box**

Utilizing CAD 3-D design files, five different shaped (rectangular, circular, triangular, hexagonal, and square). AutoCAD can generate models with accurate measurement in different scales. 3D-Printing software can efficiently use AutoCAD design files.

### **Development of wafer box using 3D- printers**

Using ABS 3mm plastic filaments and a 3-D printer, the five different shaped wafer boxes were printed for use in this research project. The ability of the 3-D printer to efficiently

use Auto CAD design files produced exact 3-D models of each wafer-box shape which contributed to the validity of research findings.

### **Voltage measurement**

Oscilloscope measured the voltage generated by PZT sensors embedded with wafer box. The wafer boxes were kept under the load wheel of the Asphalt Pavement Analyzer (APA) machine. Applying loads by the load wheels of the APA machine generated mechanical energy which was converted to the electrical power using a rectifier. The output was measured as the voltage by an oscilloscope.

### **Results and discussions**

Collected data were analyzed by applying these different statistical methods hypothesis testing, analysis of variance (ANOVA), Tukey HSD test, and Scheffe method.

## CHAPTER

### 3 LITERATURE REVIEW

This literature review chapter summarizes the existing published knowledge related to the topic for this research project. The literature review contains knowledge from scholarly articles, books, and other sources relevant to this research study. The analysis of research topic literature includes a description, summary and critical evaluation of each source, i.e., the strengths and weaknesses. The purpose of this literature review chapter was to identify gaps or controversies in the literature and topics research.

#### 3.1 ASTM Standards

ASTM International is one of the most extensive non-profit standards developing organizations in the world. This organization offers an opportunity for the advancement and publication of worldwide voluntary consensus requirements for materials, products, structures, and services (ASTM International, 2018).



**Figure 2: ASTM International** (*ASTM International, 2018*)

ASTM volunteer members are assigned to writing committees to prepared one or more standards. Committees developed more than 12,000 ASTM standards in the 80-volume Annual Book of ASTM Standards. ASTM standards are utilized by people, organizations and other establishments worldwide. Distinctive government businesses round the sector reference them in codes, regulations, and laws; and lots of others discuss with them for steering. Anyone can submit the request to ASTM who identifies a need for standardization (ASTM International, 2018).

ASTM International standards are documents that serve to formalize procedures, rules, or guidelines for industry to take after. A record which developed within the consent of ASTM

International meeting the approval requirements of ASTM procedures and regulations, only the record can become one of ASTM International's standards (ASTM International, 2018).

#### Different types of ASTM standards

1. The test method: It is ultimate procedure that produces a test outcome. Example - D 6183-00 (2005) Standard test method for tackiness of finish on leather (UMass Amherst Libraries , 2017).

2. Specification: This is the unequivocal set of prerequisites. This is required to be fulfilled by a items, item, framework, or service. Example: D 6183-00 (2005) standard test method for tackiness of fins a test result (UMass Amherst Libraries , 2017).

3. Guide: This is the information or series of options that does not recommend a explicit course of action. Example: F 893-05 Standard guide for inspection of amusement rides and devices (UMass Amherst Libraries , 2017).

4. Practice: This is the set of instructions for performing one or more specific operations that do not produce a test result. Example: F 1468-04a standard practice for evaluation of metallic weapons detectors for controlled access search and screening (UMass Amherst Libraries , 2017).

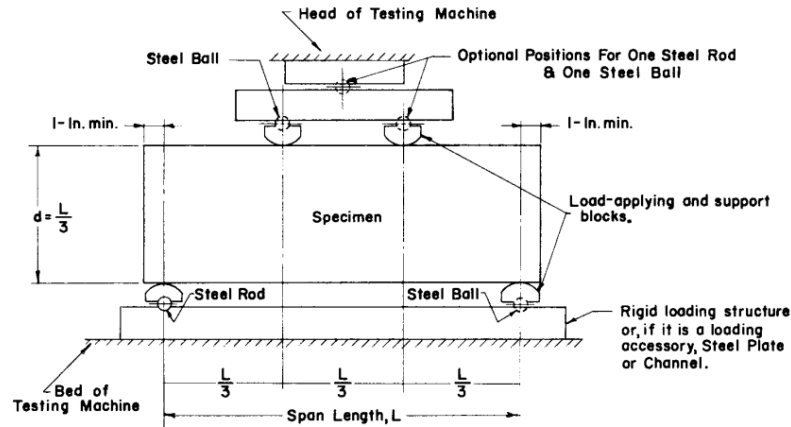
5. Classification: An efficient course of action or division of materials, items, frameworks, or administrations into groups based on comparative characteristics such as beginning, composition, properties, or utilize. Example: D 2000-05 standard classification system for rubber products in automotive applications (UMass Amherst Libraries , 2017).

6. Terminology: A document defining terms; explanations of symbols, abbreviations and acronyms. Example: F 1107-04 standard terminology relating to snowboarding (UMass Amherst Libraries , 2017).

In the literature review for this research project, it was conducted several materials such as concrete, asphalt, plastic, and electronic materials. Thus, it was focused on studying ASTM standards related to these materials.

### 3.1.1 Standard test method for flexural strength of concrete (using simple beam with third-point loading)

The test method described in ASTM C 78 – 02 covers the determination of the flexural strength of concrete using a pure beam with third-point loading. Following this method, flexural strength of specimens could be determined and the final result is report is stated as modulus of rupture (ASTM C 78 , 2002).



**Figure 3: Diagrammatic view of a suitable apparatus for flexure test of concrete by third-point loading method (ASTM C 78 , 2002)**

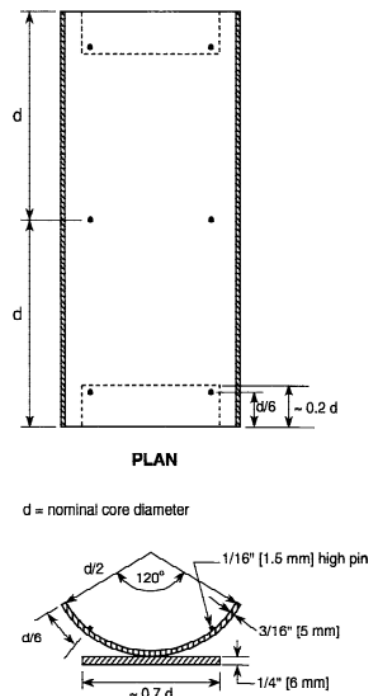
The results of this test strategy may be utilized to decide compliance with determinations for proportioning, blending and situation operations. It is utilized in testing concrete for the development of slabs and pavements (ASTM C 78 , 2002).

### 3.1.2 Standard test method for obtaining and testing drilled cores and sawed beams of concrete

The test method described in ASTM C 42/C 42M – 03 covers two tests. One is cores drilled from concrete top for compressive strength or splitting tensile strength determinations. Second test is to use sawed beams of concrete for flexural strength determinations. This test method depicts procedures for testing specimens to determine the compressive, splitting tensile, and flexural strength of concrete. Concrete bottom is stronger than the concrete top. Core strength is effected by core orientation relative to the horizontal plane of the concrete as placed. Strength is lower when measured parallel to the horizontal plane. The strength is also measured by distribution of moisture amount in the specimen during test period. The moisture conditioning procedures provide reproducible moisture environments. The procedure can be effected by some



factors as strength level of the concrete, strain characteristics, the temperature and moisture condition. (ASTM C 42/C 42M – 03, 2003).



**Figure 4: Suitable capping device for splitting tensile strength test (ASTM C 42/C 42M – 03, 2003)**

### 3.1.3 Splitting tensile strength of cylindrical concrete specimens (ASTM C-496)

The test method determines the splitting tensile strength of cylindrical concrete specimens. A diametric full force is applied along the cylinder length until failure occurs. The applied load creates tensile stresses on the surface. High compressive stress is created on the plane around the applied pressure. Due to the load area is in a state of tri-axial compression, tensile failure occurs instead of compressive failure. This result allows bearing much higher compressive stresses than uniaxial compressive strength. The obtained splitting tensile force is greater than direct tensile strength. On the other hand, splitting tensile strength is lower than flexural strength. To design lightweight concrete structures the obtain tensile strength is used. Tensile strength used to evaluate the concrete provided shear resistance. The length of reinforcement is determined by tensile strength. (ASTM C 496/C 496M, 2004).

### **3.1.4 Mounting piezoelectric emission sensors**

A sensor is a device which can detect the motion of the particles in the device using an elastic wave to transform an electrical signal. A mounting sensor is a device that holds the sensor in the structure. In the mounting method, the sensors are attached fixed on the structure to ensure the coupling of structure and sensor constant. There are few methods of mounting sensors like compression and bonding. In compression method the force to the sensor is applied by springs, torqued screw threads, magnet tapes or elastic bands, by bonding method, the sensor is fixed with the structure suitable adhesive which acts as couplant. Conducting surface needs to be kept cleaned to increase the acoustic wave detection which loses the possibilities of losing energy transmission caused by paint coatings, oxides, etc. Surface roughness is essential characters determining acoustic energy. Couplant should be corrosion resistant. There should be no voids in couplant and unevenness should be avoided. Viscosity is essential factor couplant. Liquids or greases will work as a couplant if they wet the surfaces of both the structure and the sensor. Very high viscosity couplant or a rigid bond is recommended (ASTM E650, 1997).

The mounting fixture should be designed to avoid blocking block out a substantial amount of acoustic energy from any direction. Environmental protection should be provided for the sensor or sensor and mounting fixture. The mounting fixture should be designed to have a minimum effect on the response characteristics of the sensor (ASTM E650, 1997).

Waveguide is used to prevent undesirable contact between the sensor and the structure caused by adverse contact. To prevent this, an acoustic waveguide may be used which would carry the acoustic signal from the structure to the sensor. To avoid the surface contact with material an acoustic waveguide should be mounted. It would reduce the signal damping (ASTM D 618, 2000).

### **3.1.5 Standard test method for tensile properties of plastics (ASTM D 638 - 02a)**

Following standard test method for tensile properties of plastics, the tensile property is produced for the control and specification of plastic materials. Tensile features may differ depending on speed and environment of the testing method of testing for preparation of material is an ancestor to the way of testing the material. The maximum degree of uniformity preparation, treatment, and handling should be maintained for referee purposes or comparisons within any

given series of specimens. The rate of application of stress, temperature, previous history of the sample, etc. are determining characteristics on which the exact stress-strain of plastic materials are highly dependent. Applying uniaxial tensile force to a solid material, the stretch occurs in the direction of the applied force. Poisson's ratio is used for structural designs in which all dimensional changes resulting from the application of force need to be considered (ASTM D 638, 2002).

### **3.2 UL Global standard**

UL is a worldwide autonomous safety science company with more than a century of enhancing safety arrangements from the open selection of power to new breakthroughs in sustainability, renewable energy, and nanotechnology. Devoted to advancing secure living and working situations, UL makes a difference to protect individuals, items, and places in vital ways, encouraging exchange and giving peace of intellect. UL certifies, validates, tests, verifies, inspects, audits, advises and educates. The UL give the information and offering assistance to clients to explore increasing complexities over the supply chain from compliance and administrative issues to exchange challenges and advertise to get the marketplace. Supported by more than a century of demonstrated safety science ability, businesses, customers and administrative specialists around the world recognize the trusted thoroughness and specialized brilliance of UL certifications. Exchange. UL have a global network who are dedicated for testing facilities and laboratories deliver innovative solutions for customers around the world. UL give customers a clear and expert assessment of products to determine quality, reliability and compliance. With more than a century of specialized ability in testing and creating security measures, UL has a quick understanding of existing and rising threats that can adversely influence the notoriety of a trade and the security of individuals. UL work closely with clients to explore these challenges each day. UL standards are usually distinguished as measures for security and cover sensibly predictable dangers related with an item (UL INC, 2015).

UL Standards are intended to (UL INC, 2015):

- Identify the requirements to investigate the products and provide consistency in the application requirements.
- Guide the manufacturers to develop products.

- Provide nationally recognized compatible installation code requirements.

### **3.2.1 Standard for supplementary protectors for use in electrical equipment**

This standard is applied to additional protectors for using as uneven voltage protection within electrical equipment. The acceptability of a protector for any application depends on the conditions that come over in actual service. A protector may be effected by the requirements of the equipment. There is a necessity to evaluate performance characteristics that are not specified in this standard (UL 1077, 2015).

The standard for Laboratory Hoods and Cabinets: These requirements applied to laboratory hoods and cabinets for providing an enclosed countertop work area. The work area is equipped with exhaust for containment and removal of vapors, mists, gases and particulate matter from the laboratory. (UL 1805, 2002)

### **3.2.2 Safety Requirements for electrical equipment for measurement, control, and laboratory use**

Electrical laboratory equipment has different functionalities, for example measuring, monitoring or inspecting materials use tin the production of equipment or other materials. This standard also includes non-measuring equipment such as signal generators, measurement standards, power supplies for laboratory use, transducers, transmitters, etc. This standard guides to reduce the hazards possibilities to the operator and the laboratory reduced to a tolerable level (UL 61010-1, 2016).

Requirements for protection against types of hazard are as follows (UL 61010-1, 2016):

- a) Electric shock or burn
- b) Mechanical hazards
- c) The spread of fire from the equipment
- d) Excessive temperature
- e) Effects of fluids and fluid pressure
- f) Effects of radiation, including lasers sources, and sonic and ultrasonic pressure

g) Liberated gases, explosion and implosion

### **Normal environmental conditions**

The equipment to be designed safe under the following conditions (UL 61010-1, 2016):

- a) Indoor use.
- b) Altitude up to 2000 m.
- c) Temperature 5 °C to 40 °C.
- d) Maximum relative humidity 80 % for temperatures up to 31 °C decreasing linearly to 50 % relative humidity at 40 °C.
- e) Main supply voltage fluctuations  $\pm 10$  % of the nominal voltage.
- f) Temporary overvoltage occurring on the mains supply.

### **Extended environmental conditions**

The equipment to be designed safe under the following conditions also (UL 61010-1, 2016):

- a) Outdoor use
- b) Altitude above 2000 m
- c) Ambient temperatures below 5 °C or above 40 °C
- d) Relative humidity above 80%
- e) Main supply voltage oscillation  $\pm 10$  % of the nominal voltage

The UL 61010-2-12 describes safety requirements for electrically powered laboratory equipment for the materials. Heating is one of the major functions of these electrical equipment. A refrigerating system that combines heating and cooling functions generates additional severe hazards than if those functions operated distinctly. The materials which produce significant heat into the refrigerating system that the cooling system in the application yield severe hazards risks than if operated alone (UL 61010-2-12, 2017).

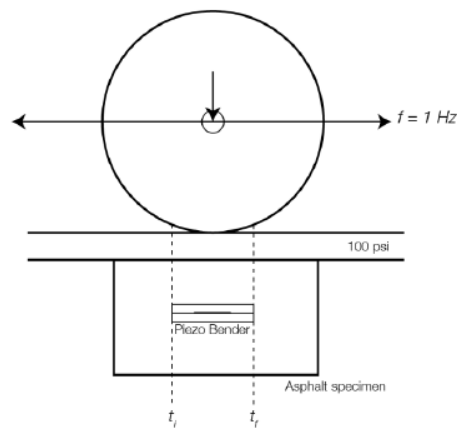
UL 61010-2-30 contains safety requirements to test and measure circuits which are connected for test devices or circuits outside the measurement equipment. The measurement

circuits are part of measurement equipment, laboratory equipment, process control equipment etc. The existence of these circuits in equipment requires additional protective means between the circuit and an operator. These circuits could measure voltages, temperature, and force via a strain gauge and Put a voltage into a circuit to study a new design (UL 61010-2-30 , 16).

UL 61010-2-33 specifies safety requirements for meters. The meters measure voltage on a circuit. They have various names given to this equipment as multimeter, digital multimeter, voltmeter, clamp meter (UL 61010-2-33, 2014).

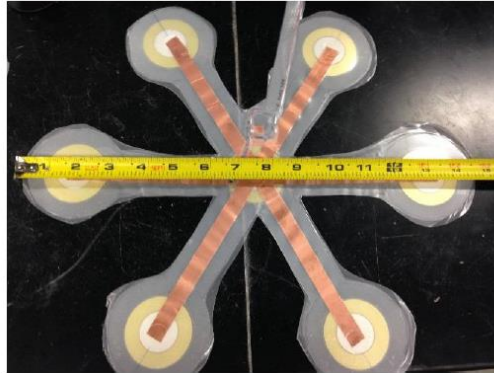
### 3.3 Case study of energy harvesting using PZT sensors

Evaluating the technical feasibility of incorporating piezoelectric systems into roadways was the primary goal of this research project. A loaded wheel test (LWT) was accomplished using an Asphalt Pavement Analyzer (APA.) for structural characterization by measuring generated voltage. In the methodology, a loaded wheel test (LWT) in an Asphalt Pavement Analyzer (APA) performed the task of simulating real road conditions under pavement (Kim et al., 2018).



**Figure 5: A Loaded Wheel Test (LWT) (Kim et al., 2018)**

In this case study, the research team tested a piezoelectric product with 100 lbs. loads in different HZ values including 30 HZ. Here HZ values can be referred to as frequency of force applied to samples. The contact area of the load wheel was approximately six square inches, and the depth of piezo elements was 2 inches from the top. The size of the sample was 6 inches in diameters and 3 inches in thickness (Kim et al., 2018).



**Figure 6: Sensors embedded in asphalt and concrete** (Kim et al., 2018)

### **Voltage and power testing with samples**

In this lab experiment PZ samples were embedded in asphalt, concrete composite, and ECC concrete, respectively. Power (voltages) from the PZ materials were measured under simulated traffic loads conditions using the APA. To develop a real traffic condition, the experiment was conducted under the assumption of 600 vehicles per hour at 45 mph. The load was 100 lbs. from each vehicle. The test ran for 8000 APA cycles which lasted for 4 ½ hours. In case of asphalt, constant decreasing voltage indicated a direct correlation with material deformation and the voltage drop (Kim et al., 2018).

### **Results of the test**

Statistical analyses, descriptive statistics, and One-way ANOVA test results indicated that the PZ system embedded in the ECC concrete was the lowest producer of power than asphalt. Flexible roadway materials (asphalt) have more electric potential than rigid materials such as composite concrete and ECC. The composite concrete produced higher values than ECC. So, it could be concluded that the magnitude of energy may be more related to strength and density than elasticity, especially in the rigid material. The deformation in asphalt is correlated to the extent of energy harvesting although deflection was not as significant as deformation (Kim et al., 2018).

### **3.4 Factors affecting piezoelectric energy harvesting**

There are several factors which effect piezoelectric energy production. There are some critical factors given below.

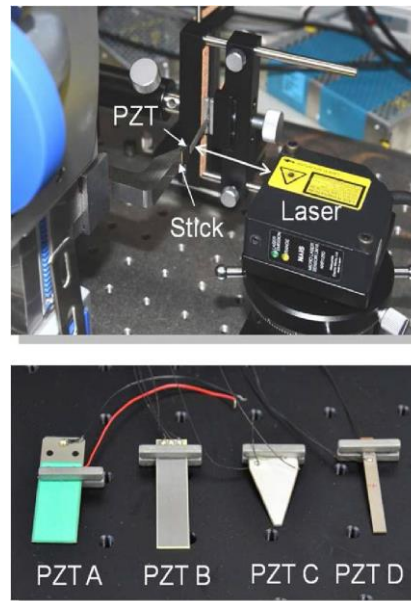
### 3.4.1 Thickness-Area ratio

The magnitude of PZT generation is the function of the ratio of thickness to the area of the material. Increasing this ratio will increase higher output. Optimum power is a function of force limitation and stress limitation.

When the material thickness is constant and if no restriction applied to the force, power will be produced at the expense of force applied to the cross-sectional area. The volume increase is a scaling factor of PZT peak power. Volume increase can be done in two ways. One is by increasing surface area and the other is by increasing thickness (C. Keawboonchuay, 2003)

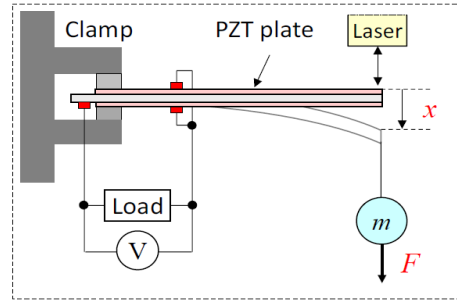
### 3.4.2 Shape Effect of Piezoelectric Energy Harvester on Vibration Power Generation (Case study 1)

The shape of devices, concentrated mass, and forced vibration have a certain effect on energy regeneration efficiency of PZT devices. A triangular plate of a PZT device showed higher regeneration efficiency than the rectangular plate's efficiency (Basari et al., 2014).



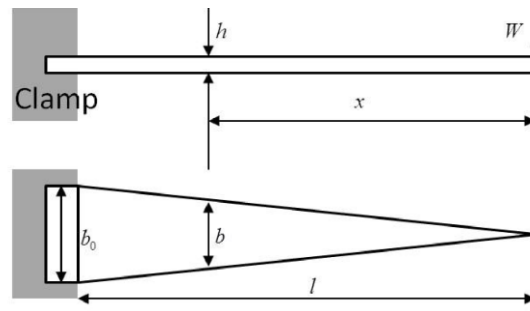
**Figure 7: Experimental setup and PZT devices** (Basari et al., 2014)





**Figure 8: Experimental setup for energy measurement** (Basari et al., 2014).

PZT devices A and C which have different shapes were used. The curvature of PZT device C is a constant value when a concentrated load is applied. PZT C had doubled deflection angle than PZT A, the input energy of PZT C is 1.5 times of that the PZT device A has.



**Figure 9: Triangular plate size specification** (Basari et al., 2014)

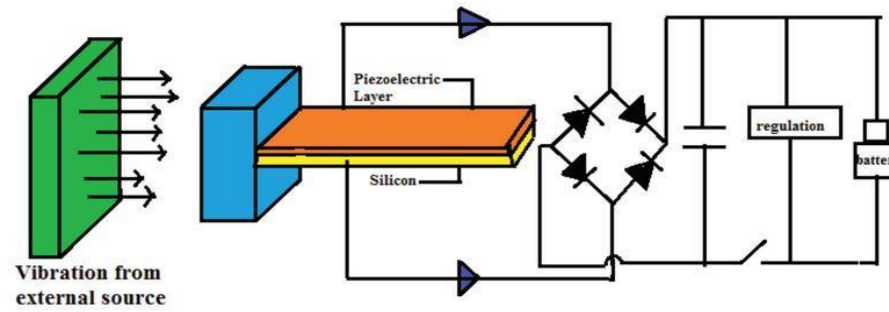
### Shape effect on same PZT area

The evaluation of shape effects of PZT devices shown in Figure 8. Those PZT devices were attached to the same size of rectangular and triangular plates. Experimental analyses with step signal input were conducted first. Second, the matching impedances for maximum power and energy generation were determined.

With the resonant frequencies of 185 Hz and 372 Hz, the triangular plate generated maximum energy. The power is power is generated highest with 4 k $\Omega$  and 2 k $\Omega$  matching impedances. The resonant frequency for the rectangular plate was 104 Hz while its matching impedance was 10 k $\Omega$ . The matching impedances for the triangular plate are smaller than the rectangular plate as the resonant frequencies of the triangular plate are higher than the rectangular plate (Basari et al., 2014).

### 3.4.3 Shape Effect of Piezoelectric Energy Harvester (Case study 2)

This case study provided a new method of power generation by designing and operating various shapes of cantilever beams (Pi, Rectangular, E, and T) with a layer of piezoelectric materials. This combination approach allows power to be generated for diverse application to replace the traditional power sources by piezoelectric energy harvester (Kaur et al., 2016).



**Figure 10: Power generator circuit** (Kaur et al., 2016)

The whole processing of a cantilever-shaped microscale device was composed of two layers, piezoelectric layers, and a semiconducting layer. The bottom layer and top layer are made up of Silicon and piezoelectric material respectively. The primary process of power generation involves energy source, energy conversion circuit, and the capture circuit. The conversion chain starts with mechanical vibrations sourced from the environment. The vibrations from the cause movement and deflection in the cantilever. The deflection in the cantilever exerted by force provides by vibration in micro-Newton. An increase in deflection with a decrease in spring constant leads to a corresponding rise in generated piezoelectric voltage. (Kaur et al., 2016).

### 3.4.4 Temperature effect on piezoelectric energy harvesting

When increasing the temperature at different loading conditions the output voltage decreases accordingly (Pasha, 2016). The research by *Mane et al.* described many factors effecting a typical response to voltage or Power of PZ materials. The three-main elements of temperature ( $T$ ), pressure ( $p$ ) and frequency ( $f$ ) were included in the analyses (Mane et al., 2012).

The temperature effect on the energy harvesting property of a pre-stressed piezoelectric thunder diaphragm was simulated. The diaphragm was vibrated at various frequencies and temperatures under a specific pressure setup. When pressure was applied, the diaphragm was pushed, and when the pressure was released, the membrane came back to its rest position which remained constant. The model data indicated that temperature has an adverse impact on the

generated voltage if there exists certain interaction with other factors, which may influence the output. This model indicated that temperature does not have a direct effect on the energy. In an interaction with other factors, the temperature was having an adverse impact leading to lower power (Mane et al., 2012).

### **3.5 Experimental research design**

An experiment is a process of study that results in the collection of data. The results of tests are unknown in advance. Statistical analyses are conducted on the data collection results. They are mathematical tests that the researcher doesn't manipulate. Such manipulation would result in biased results. It's the experimental design that the investigator manipulates according to the nature of the research, e.g., control group & treatment group; independent & dependent variables. Planning an experiment correctly is very important for ensuring the right type of data and sufficient sample size for answering the research questions of interest clearly and efficiently (Lind D., 2015).

Designing an experimental research study requires completion of the following steps:

- Defining the assessing problem and the questions.
- Defining the population of interest.
- Determining the need for sampling.
- Defining the experimental design.

Before data collection begins, specific questions that the researcher plans to examine must be identified. Besides, a researcher should identify the sources of variability in the experimental conditions. One most essential objectives of an experimental design is to segment the impacts of the roots variations of particular components to look at particular questions of interest. The objective of created research information collection strategies is to improve the accuracy of the outcome to investigate the research hypothesis (Six Sigma, 2016).

#### **3.5.1 True experimental design**

True experimental designs identify where analysts have total control over unimportant factors and can foresee certain the impact on the dependent variable due to the control of the autonomous variable (CIRT, 2018).

A true experimental research design must essentially consist of the following characteristics:

- Manipulation
- Control
- Randomization

Manipulation is control of the independent variable by the researcher through handling to identify its consequences on dependent variable (CIRT, 2018).

Control refers to use of a control group and controlling the effects of extraneous variables on the dependent variable. The subject in the control and experimental groups are similar in number and characteristic, but the subjects in the control group receive no experimental treatment or any intervention. The experimental group receives the planned treatment or intervention and a comparison is made with the control group to observe the effect of this treatment or intervention (CIRT, 2018).

Randomization means that every subject has an equal chance of being assigned to experimental groups. Probable biases are eliminated by utilizing random assignment of subjects or objects. Randomization is used for true experimental research design to diminish the risk to internal validity of the study. Randomization process also eliminates the effect of extraneous variables on dependent variables (Wikipedia, 2016). Through randomization, the characteristics of subjects in experimental and control groups are similar and represent the general average populations of interest to the researcher. Through this process of dispersing the variability of subject characteristics equally in both groups, the influence of extraneous variables is greatly reduced. (CIRT, 2018).

Since it is difficult for researchers to eliminate bias using only their expert judgment, the use of randomization in experiments is common practice. Randomization is the most dependable process to create homogeneous treatment groups. This process do not allow any likely biases. Objects are assigned to random groups for performing completely randomized design. In each treatment group, the subjects are labeled. Then subjects are selected from the table of random numbers (Yale University, 1997).

When experimenters have proper knowledge about specific differences among groups, they can use a randomized block design as a completely randomized design. For making a block design,

experimental objects are assigned into similar blocks before being assigned to a random treatment group. (Yale University, 1997).

### **3.6 Summary of Literature Review**

A review of current literature related to the topic of this research study has provided a critical insight into the most current practice as well as deficit areas in need of continued research. It also helps to identify the strengths and weaknesses of previous work.

It was evaluated several possible materials for use in this study plastic, concrete, asphalt and electronic materials. For each of these four types of materials the appropriate ASTM standards were selected so that each material would be correctly assessed for material property analysis. The ASTM standards (ASTM C-496, ASTM C39, ASTM C 642 – 06) related to concrete property, discuss the strength testing (compressive, tensile, density and void) procedures of concrete.

Mounting PZT emission sensors is a device that holds the PZT sensors in the structure. It was ensured that the coupling of structure and sensor was constant. Size, sensitivity, response, environmental and material compatibility are vital parameters to be considered when selecting sensors. To avoid undesirable contact between the sensor and the structure an acoustic waveguide may be used which would carry the acoustic signal from the structure to the sensor.

In this chapter, several UL standards have been mentioned related to lab safety. Essential standards are like safety requirements for electrical equipment used for measurement, control, and laboratory use period

The Load Wheel Test (LWT) concluded that asphalt generates the highest average voltage while embedded with PZT sensors (Kim et al., 2018). The magnitude of PZT generation is the function of the ratio of thickness to the area of the material. Increasing this ratio will increase higher output (C. Keawboonchuay, 2003).

The shape of PZT sensors has an inevitable impact on energy production of PZT materials. The triangularly shaped sensor produced more electricity than rectangular shaped PZT sensor of the same area (Basari et al., 2014).

### 3.7 Controversies of some research papers

In the paper by *Kaur et al.* it has been shown the shape effect of PZT materials on energy harvesting. The experiment result showed that E shaped produced the highest energy when compared to the other shaped elements. But this experiment is questionable because all the shapes did not have the same mass. Thus, it is difficult to conclude E shape has the most positive effect on electricity production.

In the paper by *Mane et al.* the temperature model indicated that temperature does not have a direct effect on the energy. But they also said that, in an interaction with other factors, the temperature is having an adverse impact leading to lower power which contradicts the author's research conclusion.

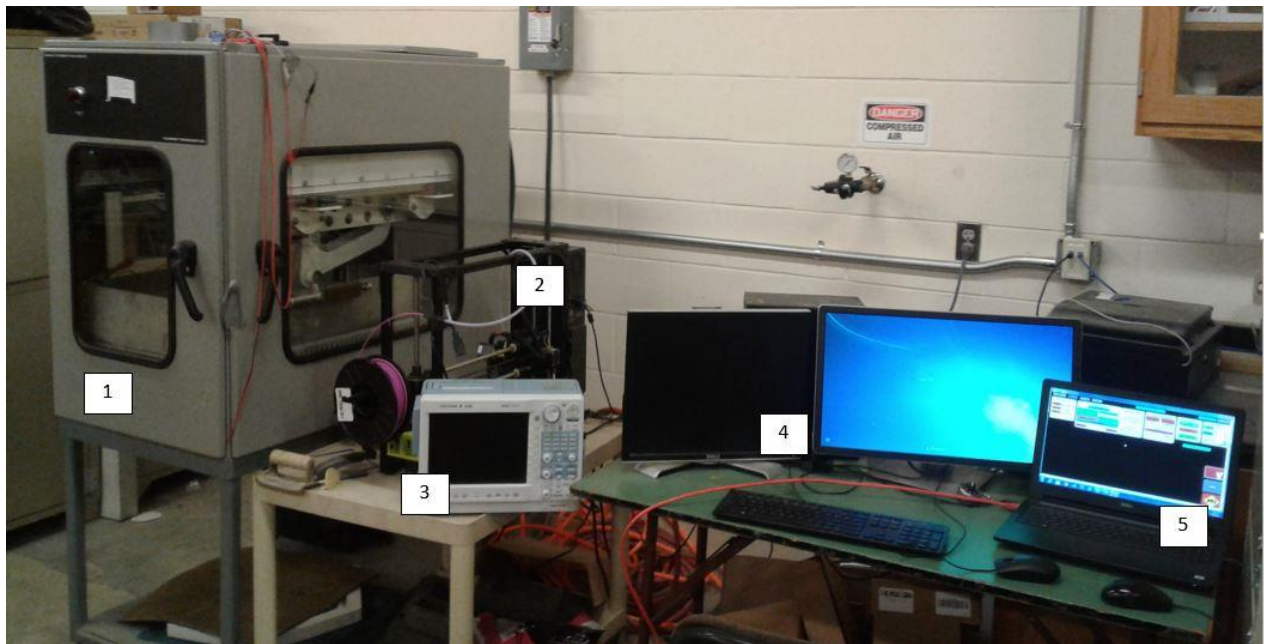
## CHAPTER

### 4 METHODOLOGIES

This chapter discusses the methods of the research. The primary purpose of this research was to develop different shaped wafer-boxes using 3D-printer. It was identified if there exists any shape effect of wafer box on energy (voltage) harvesting. To achieve the objectives, different lab experiments were conducted. Before running lab experiments, lab setup and proper experiment design are two of the most important tasks. When conducting lab experiments, voltage data was collected. The collected data would be analyzed using different statistical tools to identify the outcome.

#### 4.1 Equipment for testing

To achieve the research objectives one by one, it was essential to essential to correctly design each experiment. For conducting experimental research or data collection, a good lab set-up was important. Equipment for the research project include an APA (Asphalt Pavement Analyzer) machine, electronic oscilloscope, a Lulzbot TAZ6 3D-Printer, lab computer, and tools.



**Figure 11: Lab arrangement (From Left 1. APA machine, 2. 3D-printer 3. Oscilloscope, 4. Lab computer, 5. APA control computer)**

In this chapter, each piece of equipment for the research project has been discussed in detail. Equipment used in this research study are as follows:

#### 4.1.1 Asphalt Pavement Analyzer-Junior (APA Jr.)



**Figure 12: Asphalt Pavement Analyzer-APA Jr.**

APA-Jr is a tester with a multifunctional loaded wheel which can evaluate cold and hot asphalt mix in a dry or submerged water condition. It can do tests for following types of samples:

##### 1. Cylindrical

- Gyrotory
- Marshal
- Hveem
- Roadway cores
- Other cylindrical samples

##### 2. Beam

- Vibratory
- Rolling wheel
- Slabs
- Other beam samples

The APA-Jr. Has four loaded wheels

- APA concave



- Hamburg-type
- Solid rubber
- APA solid steel

The APA Jr. is designed to meet the provisions of AASHTO TP63-06 Test method for determining the rutting susceptibility of hot mix asphalt and the requirements of AASHTO T324-04 test method for Hamburg- type wheel tracking test. The PLC-PC based control system runs the APA-Jr.. The operating system of APA allows a user to perform all calibrations and functions directly with a computer.

**Table 1: APA (Asphalt Pavement Analyzer) Jr. machine specification**

Properties	Measures
Width	31 inches
Length	44 inches
Height	68 inches
Weight	1,400 Lbs.
Water tank capacity	17 gallons
Power requirements	204 or 240 VAC, 50/60HZ, 60Amp, Single Phase
Air requirements	120PSI minimum.



**Figure 13: Advanced Pavement Analyzer inside arrangement (APA) Jr.**

### 4.1.2 Oscilloscope



**Figure 14: Yokogawa DL850V scope-corder(Oscilloscope)**

In this research project to measure energy (voltage), a Yokogawa DL850V scope corder was used. The DL850 ScopeCorder Series are modular, waveform recording instruments that can measure voltage, current, strain, acceleration, and other phenomena simultaneously. With high-speed sampling, high isolation withstands voltage, and multichannel measurements, the DL850 Series offers robust support in the development, evaluation, and quality control of energy efficient devices. It can perform different statistical measures.

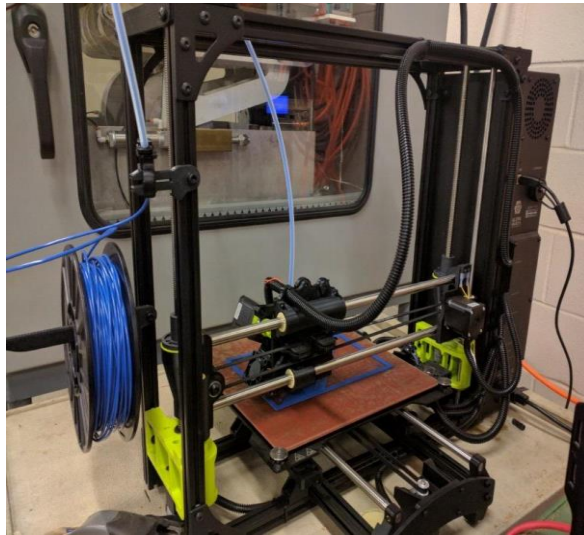


**Figure 15: Output display of the oscilloscope**

### 4.1.3 3D-Printer

3D printing provides many advantages like simplicity, reliability and precision. This is becoming widely used for making concept components. 3D-printing in research enables faster breakthroughs. Researchers are turning to 3D printing to help craft prototypes. 3D-printers can create near impossible geometries in production-grade plastics, precise forms with multiple material properties and pretty much any other materials. Three-dimensional printing makes it cheap to create a single item. One advantage of 3D printing is rapid manufacturing. Small parts can be produced within a short period and can be used instantly.

The GSU research team used a Lulzbot TAZ 6 3D Printer for this research project. This printer is compatible with different 3D printing filaments. It can 3D print with ABS, PLA filaments made from metallic, stone-like, wooden, nylon and other flexible materials. The printer can print in different printing condition based on the filament types. To operate the 3D printer for use in this study, it was necessary to install software on the computer. It was required a 3D printer host, a .STL to .GCODE generator, and optional CAD or 3-D modeling software.



**Figure 16: TAZ LULZBOT 6 3-D Printer**

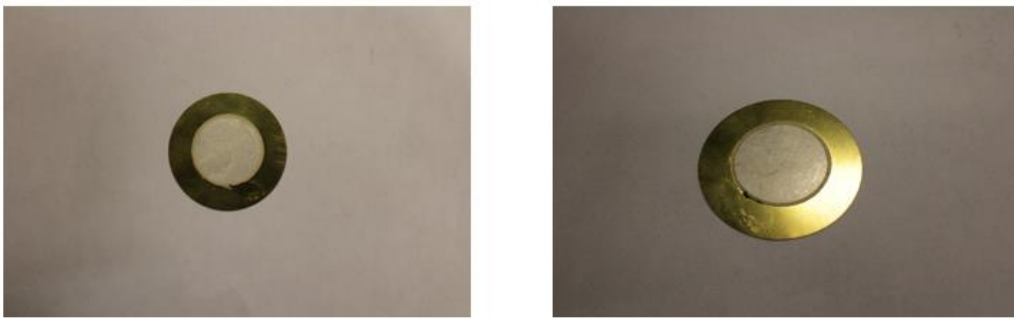
### 4.1.4 Circular Ceramic disc sensor

The PZT(Lead Zirconate Titanate) material is one of the world's most widely used piezoelectric ceramic materials. When force is applied, PZT has a perovskite crystal structure, each unit of which consists of a small tetravalent metal ion in a lattice of large divalent metal ions. The small tetravalent metal ion is usually titanium or zirconium. The sizeable divalent

metal ion is usually lead. Under conditions that confer a tetragonal or rhombohedral symmetry on the PZT crystals, each crystal has a dipole moment (APC International, 2018).

Piezoceramics are physically active, chemically inert and relatively inexpensive to manufacture. These materials can be easily tailored to meet the requirements of a specific purpose. PZT ceramic is valued because it has even higher sensitivity and higher operating temperature than other piezoceramics (APC International, 2018).

For this research project, a circular ceramic disc PZT sensor was used. In this sensor, a smaller ceramic disk is attached to the central part of the copper disk. The PZT sensor can absorb mechanical energy under different load being embedded into different types of construction or road or any types of materials. PZTs of the same kind vary with performance. The more it bends the more voltage alternately it produces due to crystal structure expanding and contracting.



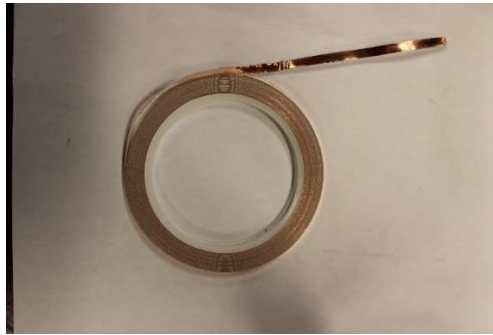
**Figure 17: Piezoelectric sensor used to harvest energy (Top view)**



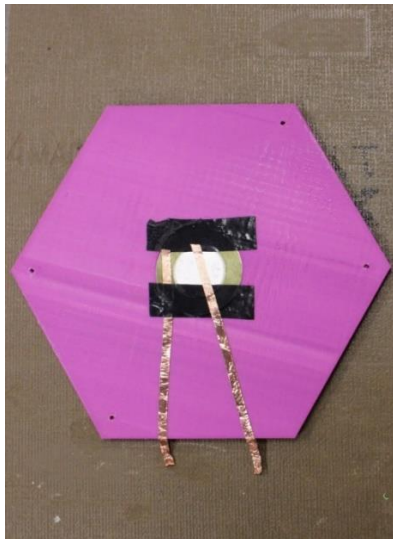
**Figure 18: Piezoelectric sensor used to harvest energy (Bottom view)**

The diameter of the sensor is 1.9375 inch, and the depth is 0.018 inch. The sensor was selected based on the previous energy harvesting experiments in the same lab where these same types of sensors were used successfully. Copper ribbons were used with the sensors to collect

harvested energy (Figure 19). There was one connection to the positive port and the negative port. The positive and negative lines could be used alternately.



**Figure 19: Copper ribbon used with the sensors in the wafer box**



**Figure 20: Ceramic disc sensor attached to wafer box with two ports (Positive and negative)**

## 4.2 Wafer box design in CAD

Different shaped wafer-box were developed to identify the effects of shape on piezoelectric energy production. For this research project the following forms were considered:

- Rectangular
- Circular
- Triangle
- Square

- Hexagonal

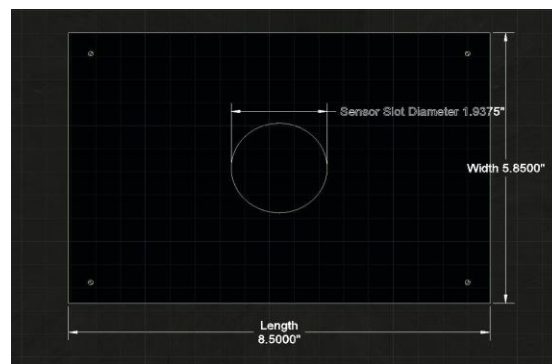
It was necessary to design different shaped wafer-boxes accurately. To perform 3-D box design, an Auto CAD 2017 version was used. Auto CAD software was used because it could perform accurate measurements and generate realistic 3D visual models. As an example, the design steps of rectangular wafer box have been given below.

Rectangular model: The rectangular shaped box had a size of half of the “Letter” sized paper. The box has two parts; one was the upper part covering the sensor, and other was the lower part holding the sensor. The dimension of the each of two parts of rectangular box is 8.5” × 5.845” × 0.25”.



**Figure 21: Upper part of the wafer box (Auto CAD 2D plan view)**

The bottom part of the box has a circular shaper slot to hold the ceramic disc sensor. The diameter of the slot is 1.9375 inches. The slot has a depth of .018 inch. This slot has been designed in a way that the sensor fits in the slot efficiently.



**Figure 22: Lower part of the rectangular wafer box (Auto CAD 2D plan view)**

There is a hollow channel in the below surface of the upper part of the box. The dimension of the channel is 0.2502” × 1.92643” × 0.17.”



**Figure 23: Hollow channel in the upper section (Top view)**



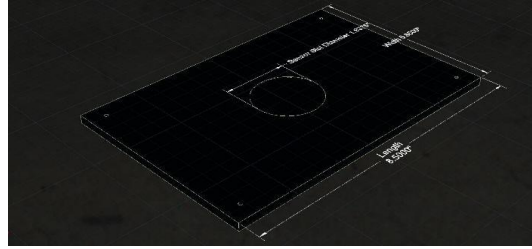
**Figure 24: Hollow channel in the upper part (3D wire-view)**

This channel passes the electric ribbon from the sensor to the rectifier. There are four screw holes to the four corners of the box. The diameter of the screw head is 0.25 inch

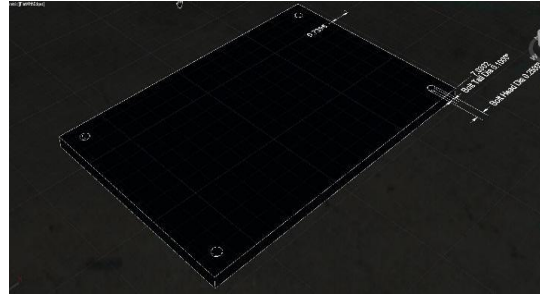


**Figure 25: Bolt dimensions**

Tail diameter is 0.1 inch. The holes have been dragged to the bottom of the sensor.

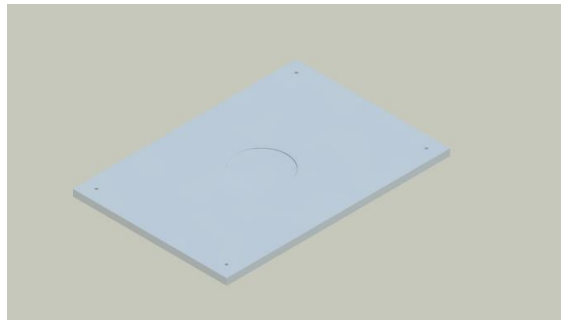


**Figure 26: Isometric view of rectangular box sensor (Bottom plate)**

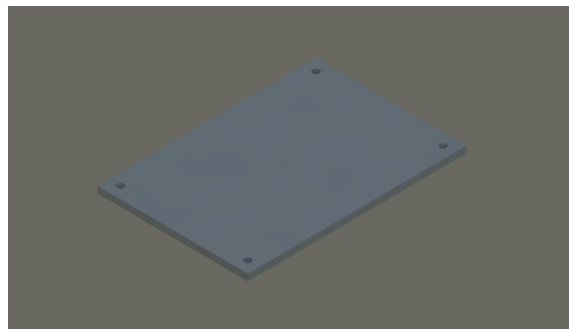


**Figure 27: Isometric view of rectangular box sensor (Top Plate)**

The 3D wire view model was rendered to realistic 3D model using Auto CAD 2017.



**Figure 28: A Realistic 3D model of wafer box (Top Plate)**



**Figure 29: A Realistic 3D model of wafer box (Bottom plate)**



### 4.3 3D-Printer for printing model wafer-box

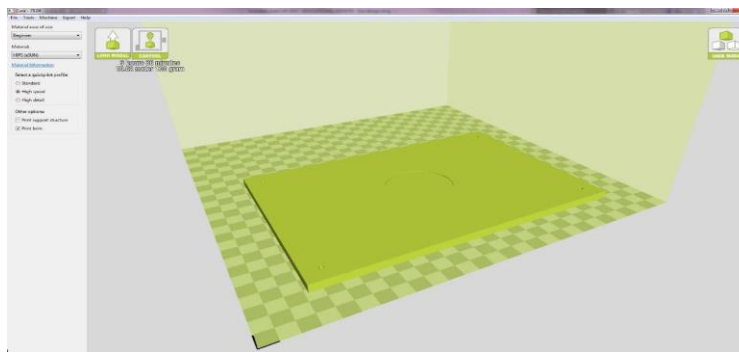
3D-printer is a modern technology device that can print any 3D objects into a real model. In this research project, the 3-D-printer has been used to print wafer-boxes utilizing the CAD design files. The printing process of a wafer-box has been described below.

#### 4.3.1 Printer hosts

Printer host is software that can be used to control the 3D printer. The program does not only allow it to move along with the axes, but also to set temperatures manually, send commands, and receive feedback or error reports related to onboard electronics. To print the model CURA 21.04 was installed in the lab PC where printing commands were given. The program took the 3-dimensional model and determined the 3D printer toolpath based on options selected. The slicing engine used the nozzle diameter, movement speeds, layer height and other variables to determine the coordinates where it needed to move. It identified the rates at which it did the printing. This information exported as a GCODE file. The GCODE file is a plain-text file with a series of text-based codes and list of complete X, Y, and Z-AXIS coordinates used for printing the 3D model.

#### 4.3.2 Printing 3D Model

The 3D design was printed in a 3D printer as the real model. In this research project, a Lulzbot TAZ6 3D-printer was used. ABS 3mm filament was used as printing material. In this research project, a Lulzbot TAZ6 3-D printer with added software, CURA 21.04 was used.

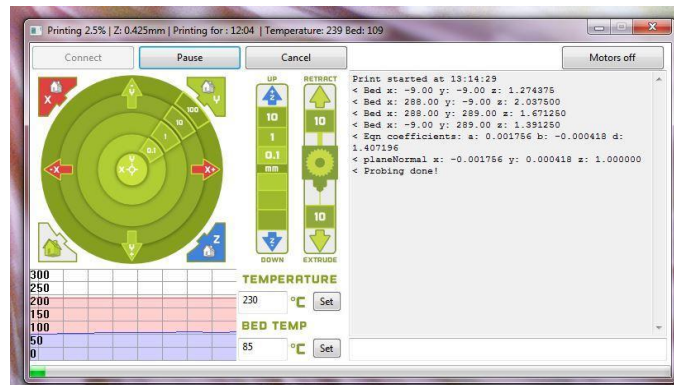


**Figure 30: File preview in the CURA 21.04 software**

The printer was connected to the CURA 21.04 software. 3mm ABS filament was loaded into the printer. The thread was inserted into the printing nozzle. As the design file was

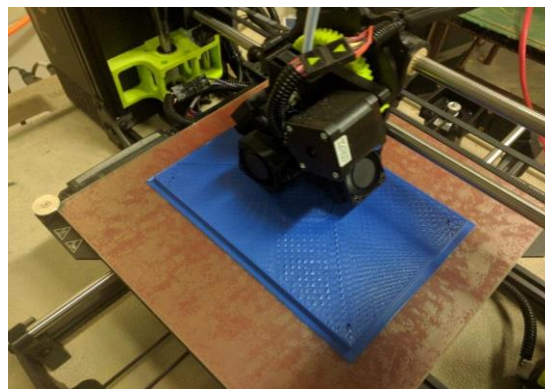
developed in Auto CAD 2017, the design file format was .dwg. But the printer could not take this format file, so it was necessary to export the data into another file format called stereolithography. The printing file was loaded into the CURA 21.04 software to be printed out.

is the 3-D printer with CURA 21.04 software can generate various surface texture quality depending on the model requirement. The printing time was controlled by using quick printing profile. High-quality printing required much more time than the lower quality.



**Figure 31: Printer host CURA 21.04 software**

The nozzle temperature could be set up to 280 degrees centigrade, and the bed temperature up to 120 degrees Celsius. The upper part of the rectangular wafer-box used 13.62m length thread weighing 108gm. Upper part took 3 hours and 36 minutes to be printed. The lower portion used 13.38m length thread weighing 106gm. Lower portion was printed in 3 hours and 30 minutes.



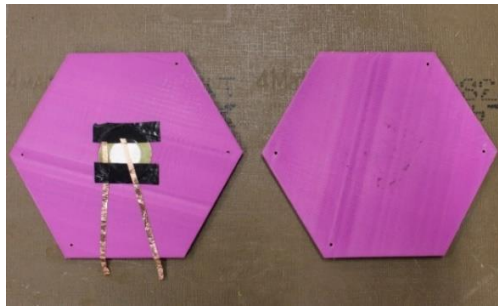
**Figure 32: Printing wafer box with 3D printer**

To print the product, ABS 3mm PLA material was used. This type of material prints at 215-235 centigrade temperature.

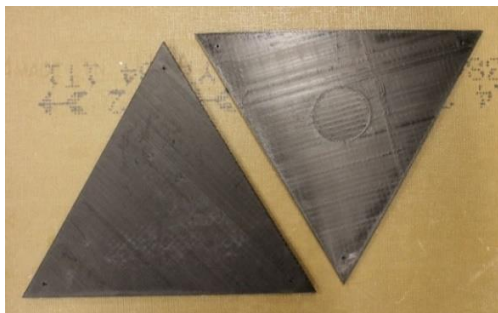


**Figure 33: 3D-Printing material (ABS 3mm PLA)**

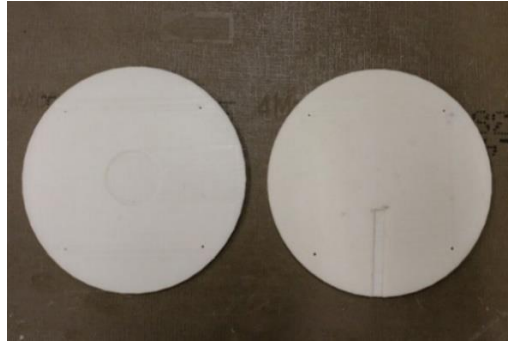
The images of five different shaped wafer boxes printed by the 3-D printer have been given below:



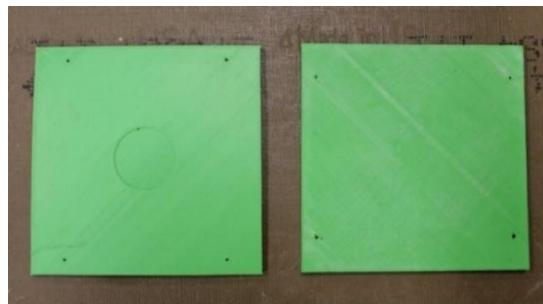
**Figure 34: Hexagonal shaped wafer box**



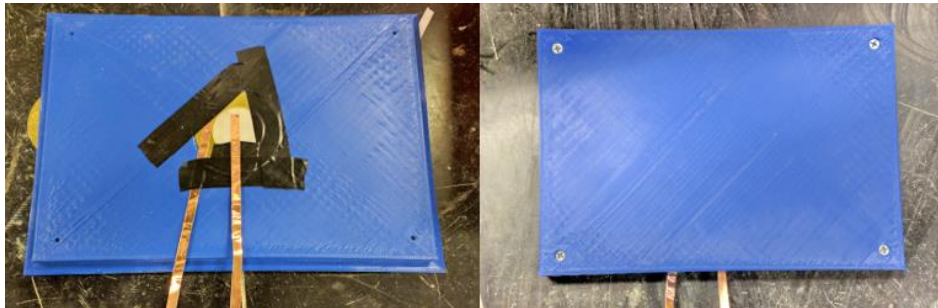
**Figure 35: Triangular shaped wafer box**



**Figure 36: Circular shaped wafer box**



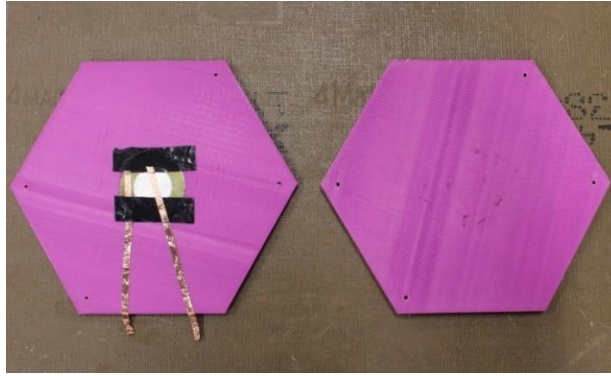
**Figure 37: Square shaped wafer box**



**Figure 38: Rectangular shaped wafer box**

#### **4.4 Embedding PZT sensor in wafer-box**

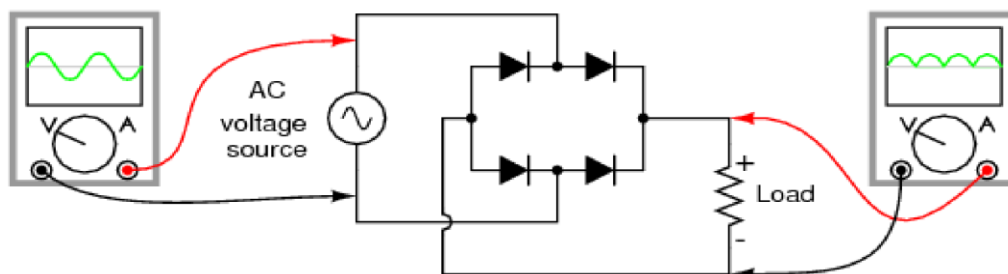
AutoCAD designed five different shaped wafer boxes. After the development of a wafer-box, a PZT sensor (circular ceramic disc) was embedded in the center of the box (Figure 39). The sensors were kept fixed in the wafer-box by scotch tape. Two copper ribbons were connected to the sensors. One of them works as positive port and the other one as a negative port.



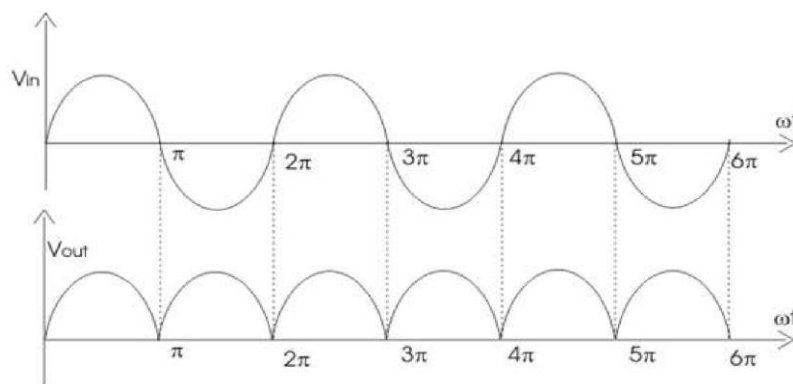
**Figure 39: Embedded PZT sensor in wafer-box**

#### 4.5 Designing circuits for recalculation of generating power and energy

The AC voltage power generated from PZT sensors needed to be converted to DC voltage. For this reason, a rectifier was used to transform AC voltage to DC output. A bridge rectifier was chosen for this purpose. Figure 40 shows the layout of a full-bridge rectifier that provided full-wave rectification. For removing the pulsating nature of the rectified output voltage, a capacitor was used to smooth out this voltage, as shown in Figure 40.



**Figure 40: A layout of the Full-wave bridge rectifier**



**Figure 41: Full Bridge Rectifier input and output voltage curves**

Power is calculated from the DC rectified voltage,  $V$ , and output load resistance  $R$  by the following equation:

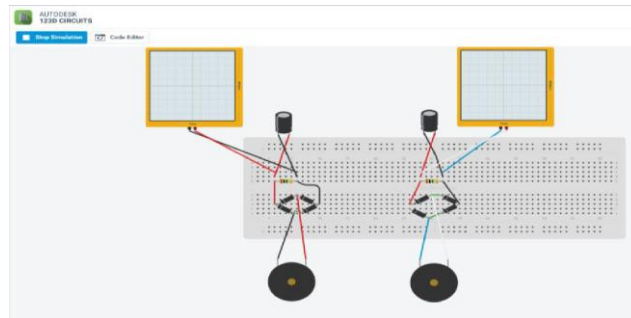
$$\text{Power (Watts)} = V^2 \div R$$

Energy can also be calculated if a capacitor is added in parallel to the resistive load:

$$E = \frac{1}{2} CV^2$$

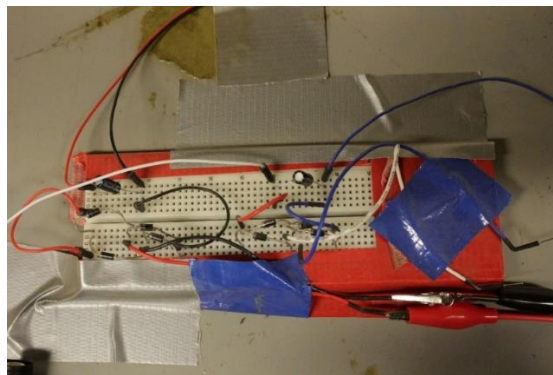
Where  $C$  equals the capacitor in Farads  $V$  is the voltage across the resistance.

The desired output determines the type of circuits used to harvest the energy from a piezoelectric transducer to the load which most often needs to be rectified, filtered, and regulated. The rectifier was designed in the APA lab on [123D.circuits.io](http://123D.circuits.io).



**Figure 42: The rectifier circuit**

A piezoelectric transducer is an AC source which is parallel with a electronic capacitor. For converting this signal into a useful one, an AC-DC converter was used to rectify the AC signal.



**Figure 43: Equipment Set-up for Testing Rectified Voltages in load**

The output from this converter was sent to a DC-DC converter where appears as the desired voltage. The direct voltage/open circuit voltage measurement was connecting the

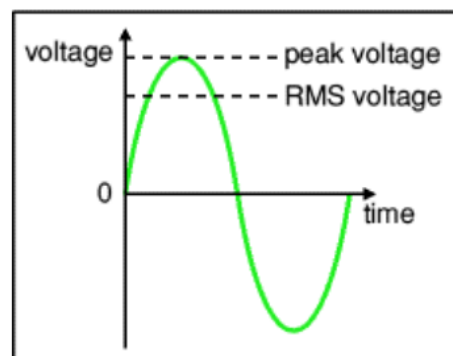
oscilloscope channel wires directly to the PZT sensor's wires. To measure rectified voltage with no loads the capacitors and resistors were taken out, the direct sensor wires were attached to the front, and the oscilloscope wires were attached to the back wires. The leftmost rectifier was used for direct loading, and the rightmost rectifier was used for indirect loading.



**Figure 44: Voltage measurement by the oscilloscope**

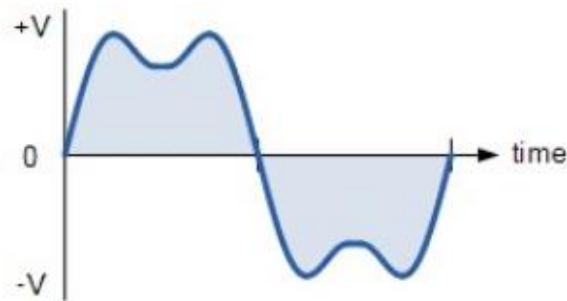
The RMS (Root Mean Square) voltage valued from the oscilloscope display was recorded as AC measure. RMS is one of the most critical parameters that is used to describe the strength of an Alternating Current (AC) (RAE, 2018).

The root means square value of a quantity is the square root of the mean value of the squared values of the amount taken over an interval. The value of an AC voltage is continually changing from zero up to the positive peak, through zero to the negative peak and back to zero again (RAE, 2018).



**Figure 45: Sine wave-AC current (RAE, 2018)**

RMS value of an AC voltage is equivalent to the DC voltage that produces the same heating effect when applied across an identical resistor. It is also a measure of energy content in each signal. Often the voltage is not smooth and linear. This non-linear curve is also referred to as non-sinusoidal.



**Figure 46: Non-sinusoidal curve** (*Macromatic Inc, 2018*)

Peak measuring and averaging does not provide an accurate measurement of these voltage conditions. The RMS value is the valid value of a varying voltage or current. It is the equivalent steady DC value which gives the same effect (*RAE, 2018*).

The equation for calculating RMS is

$$V_{RMS} = 0.7 V_{peak} \text{ (RAE, 2018)} \quad (9)$$

## 4.6 Experimental design for data collection

In this research project, it was developed two designs for the experiment. One was preliminary design, and the second was final experiment design. These two designs are described below.

### 4.6.1 Preliminary experimental design

For this experiment design five circular disk PZT sensors were randomly chosen. These five sensors were given a mark from 1 to 5 to be identified easily. The use of any sensor with the wafer box was randomly selected. The same sensor was not embedded in same wafer box for the second time. For example, if out of five sensors, one sensor was chosen randomly to be used



with a specific shaped wafer box, the second sensor would be chosen from the rest of four sensors. This way 25 combinations were made as follows:

**Table 2: Possible Combinations of PZT sensors and Wafer-box**

<b>PZT sensor mark</b>	<b>Circular wafer box:</b>	<b>Hexagonal wafer box:</b>	<b>Square wafer box: S</b>	<b>Rectangular wafer box: R</b>	<b>Triangular wafer: T</b>
P <sub>1</sub>	P <sub>1</sub> C	P <sub>1</sub> H	P <sub>1</sub> S	P <sub>1</sub> R	P <sub>1</sub> T
P <sub>2</sub>	P <sub>2</sub> C	P <sub>2</sub> H	P <sub>2</sub> S	P <sub>2</sub> R	P <sub>2</sub> T
P <sub>3</sub>	P <sub>3</sub> C	P <sub>3</sub> H	P <sub>3</sub> S	P <sub>3</sub> R	P <sub>3</sub> T
P <sub>4</sub>	P <sub>4</sub> C	P <sub>4</sub> H	P <sub>4</sub> S	P <sub>4</sub> R	P <sub>4</sub> T
P <sub>5</sub>	P <sub>5</sub> C	P <sub>5</sub> H	P <sub>5</sub> S	P <sub>5</sub> R	P <sub>5</sub> T

Using the combinations in table 2, sensors were embedded into wafer boxes to conduct load wheel test in APA machine.

#### 4.6.2 Final experimental design for final data collection

For this experiment design twenty-five circular disk PZT sensors were randomly chosen. These sensors were given a mark from 1 to 25 to be identified easily. These sensors were arranged into five blocks. Each block contained five PZT sensors. The block table is given below. To use any sensor with the wafer box was picked randomly. The same sensor was not embedded in same wafer-box for the second time.

**Table 3: Five blocks of PZT sensors**

<b>Block</b>	<b>Sensor no</b>				
<b>B1</b>	1	2	3	4	5
<b>B2</b>	6	7	8	9	10
<b>B3</b>	11	12	13	14	15
<b>B4</b>	16	17	18	19	20
<b>B5</b>	21	22	23	24	25

Using the combinations in table 3, PZT sensors were embedded into wafer boxes for using APA load wheels test.

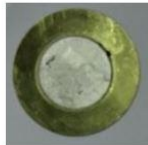



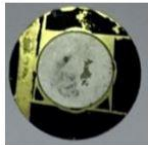
Block no	PZT Sensors				
	1	2	2	4	5
B1					

Figure 47: PZT sensors (block 1)

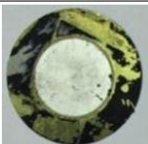
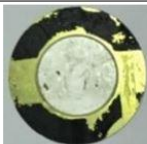

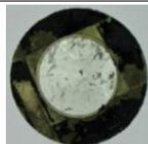
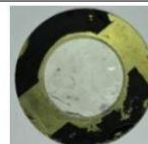
Block no	PZT Sensors				
	6	7	8	9	10
B2					

Figure 48: PZT sensors (block 2)

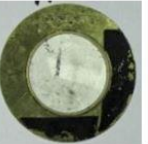
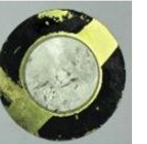
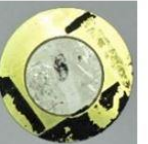

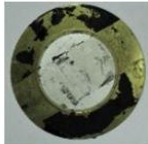
Block no	PZT Sensors				
	11	12	13	14	15
B3					

Figure 49: PZT sensors (block 3)

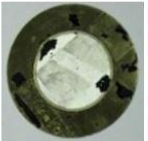
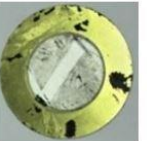

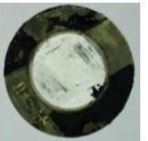
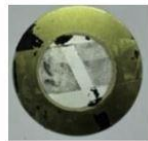
Block no	PZT Sensors				
	16	17	18	19	20
B4					

Figure 50: PZT sensors (block 4)






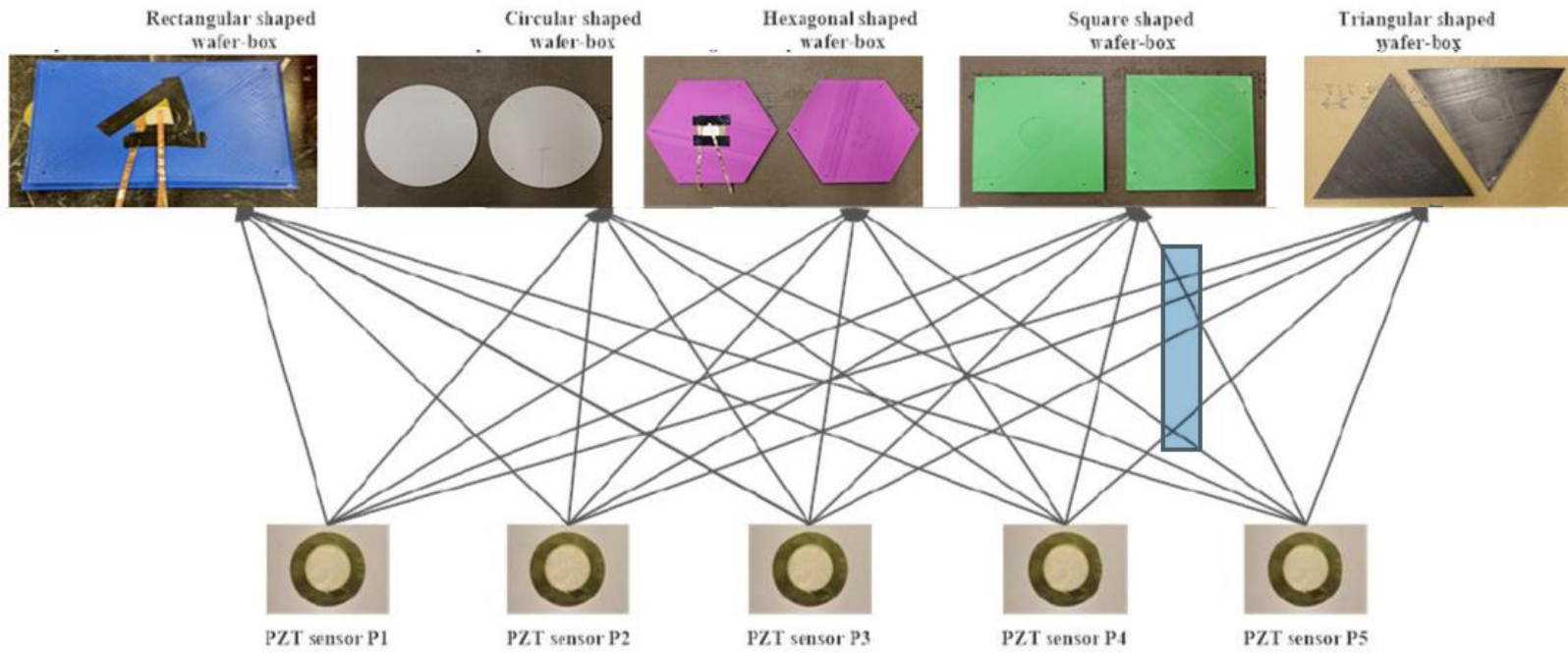
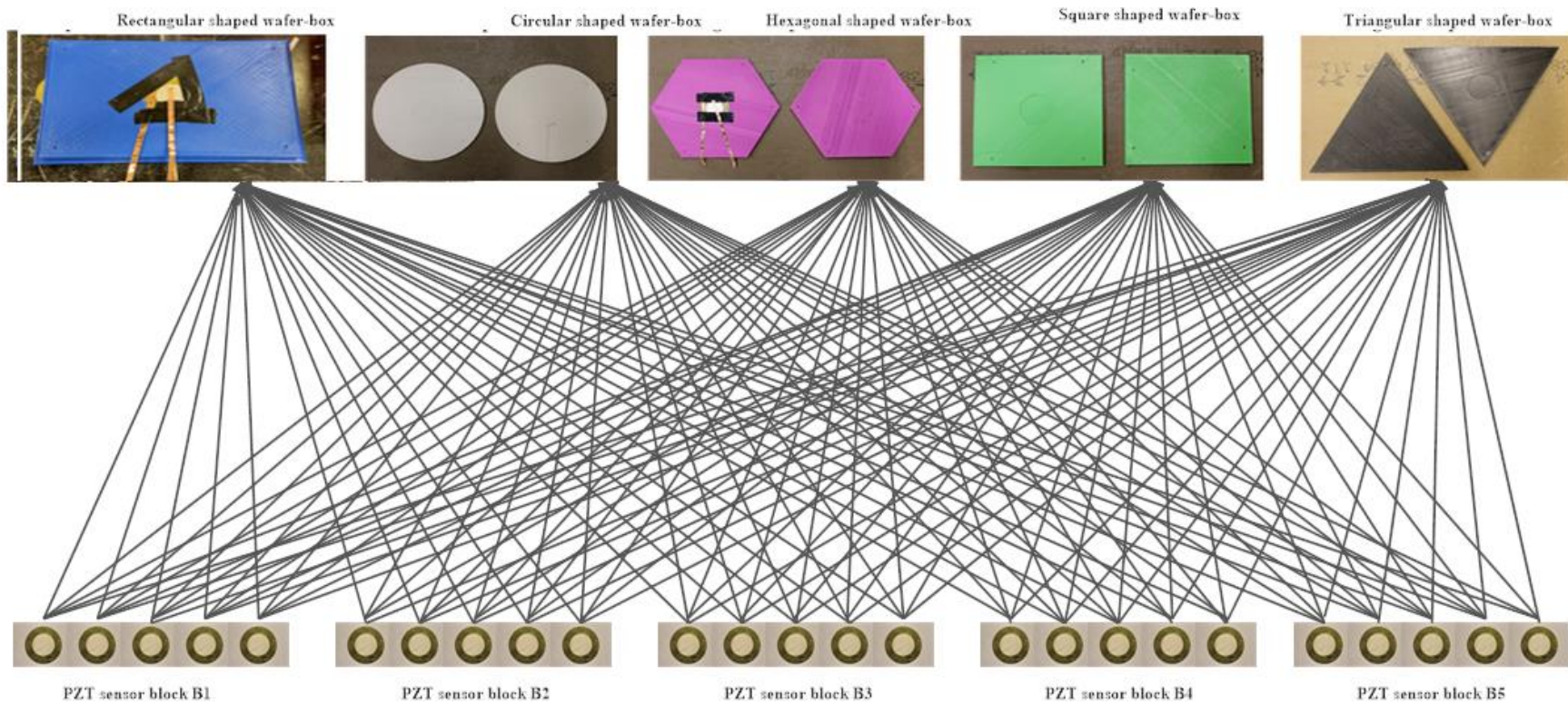
Block no	PZT Sensors				
	21	22	23	24	25
B5					

Figure 51: PZT sensors (block 5)



**Figure 52: Preliminary experimental design (Sensor- wafer box combination)**



**Figure 53: Final experimental design (Sensor- wafer box combination)**

**Table 4: Possible combinations of five different shaped Wafer box and twenty-five PZT sensors**

Sensors no according to blocks		Wafer box-PZT sensor combinations				
Block no	Sensor	Circular	Hexagonal	Square	Rectangular	Triangular
<b>B1</b>	1	C1	H1	S1	R1	T1
	2	C2	H1	S2	R2	T2
	3	C2	H3	S3	R3	T3
	4	C4	H4	S4	R4	T4
	5	C5	H5	S5	R5	T5
<b>B2</b>	6	C6	H6	S6	R6	T6
	7	C7	H7	S7	R7	T7
	8	C8	H8	S8	R8	T8
	9	C9	H9	S9	R9	T9
	10	C10	H10	S10	R10	T10
<b>B3</b>	11	C11	H11	S11	R11	T11
	12	C12	H12	S12	R12	T12
	13	C13	H13	S13	R13	T13
	14	C14	H14	S14	R14	T14
	15	C15	H15	S15	R15	T15
<b>B4</b>	16	C16	H16	S16	R16	T16
	17	C17	H17	S17	R17	T17
	18	C18	H18	S18	R18	T18
	19	C19	H19	S19	R19	T19
	20	C20	H20	S20	R20	T20
<b>B5</b>	21	C21	H21	S21	R21	T21
	22	C22	H22	S22	R22	T22
	23	C23	H23	S23	R23	T23
	24	C24	H24	S24	R24	T24
	25	C25	H25	S25	R25	T25

#### 4.7 Statistical methods used for data analysis

In this research project different statistical methods, one-way ANOVA, Tukey HSD Q test and Scheffe's method were used to analyze collected experiment data. These methods are described in detail below.

### 4.7.1 One-way ANOVA analysis

The one way analysis of variance (ANOVA) is utilized to identify substantial difference among two or more independent groups of datasets.

There are basic assumptions to ANOVA analysis

- Sample population is normally distributed
- All datasets have common variance
- Samples are drawn independent
- Observations samples are random and independent

The one-way ANOVA compares the means between the groups to determine if the means of groups are statistically significantly different from each other. It tests the null hypothesis:

$$H_0: \mu_1 = \mu_2 = \dots = \mu_k$$

Here  $\mu$  = group mean and  $k$  = number of groups. If the one-way ANOVA returns a statistically significant result, the alternative hypothesis ( $H_A$ ) is accepted where that is there are at least two group means that are statistically significantly different from each other (Lind D., 2015).

#### Test Statistic for ANOVA:

The test statistic for testing  $H_0: \mu_1 = \mu_2 = \dots = \mu_k$  is:

$$F = \frac{\sum n_j (\bar{X}_j - \bar{X})^2 / (K-1)}{\sum \sum (X - \bar{X}_j)^2 / (N-K)} = \frac{MS_{between}}{MS_{within}} = \left( \frac{SS_{between}}{df_{between}} \right) / \left( \frac{SS_{within}}{df_{within}} \right) \quad (1)$$

The critical value is found in a table of probability values for the F distribution with (degrees of freedom)  $df_1 = k-1$ ,  $df_2 = N-k$ . In the test statistic,

$n_j$  = the sample size in the  $j^{\text{th}}$  group

$\bar{X}_j$  = Sample mean in the  $j^{\text{th}}$  group, and  $\bar{X}$  is the overall mean.

$k$  = the number of independent groups

$N$  = Total number of observations in the analysis

Standard Deviation: The standard deviation is used to measure the quantity of variation of a set of data values. A low standard deviation indicates the data points which are closed to the mean of the data set, On the other hand, a high standard deviation means that the data points are spread out over a widespread range of values (Lind D., 2015).

The equation of sample standard deviation is as follows:

$$S = \sqrt{\frac{\sum_{i=1}^N (x_i - \bar{x})^2}{N-1}} \quad (2)$$

Where  $\{x_1, x_2, \dots, x_N\}$  the observed values of the sample items are,  $\bar{x}$  is the mean value of these observations, and  $N$  is the number of observations in the sample (Lind D., 2015).

The formula for the sample standard variance is

$$S^2 = \frac{\sum_{i=1}^N (x_i - \bar{x})^2}{N-1} \quad (3)$$

Where  $\{x_1, x_2, \dots, x_N\}$  the observed values of the sample items are,  $\bar{x}$  is the mean value of these observations, and  $N$  is the number of observations in the sample (Lind D., 2015).

The formula for population standard deviation is

$$\sigma = \sqrt{\frac{\sum (X - \mu)^2}{\eta}} \quad (4)$$

$\sigma$  = population standard deviation

$\mu$  = population mean

$\eta$  = number of scores in sample.

The formula for population standard variance is

$$\sigma^2 = \frac{\sum (X - \mu)^2}{\eta} \quad (5)$$

= population standard deviation

$\mu$  = population mean

$n$  = number of scores in sample

#### 4.7.2 Tukey HSD test

The Tukey's Honest Significant Difference (HSD) test, is a post-hoc test based on the studentized range distribution. An ANOVA test can tell if results are significant overall, but it does not tell exactly where those differences lie. After an ANOVA result is found to be significant, then the Tukey's HSD test can be applied to find out which specific group's means (compared with each other) are different. The test compares all possible pairs of means (ITL, 2007).

The critical value of the Tukey-Kramer HSD Q statistic is established based on the  $k$  = number of treatments and  $v$  = degrees of freedom for the error term and the significance level  $\alpha$  = 0.01 and 0.05 (p-values) in the Studentized Range (Duke University, 1998).

The next step required to establish a Tukey test statistic from sample columns is to compare with the appropriate critical value of the studentized range distribution. Parameters for each pair of columns compared are called as the Tukey-Kramer HSD Q-statistic or simply the Tukey HSD Q-statistic:

$$Q_{i,j} = \frac{|\bar{x}_i - \bar{x}_j|}{s_{i,j}} \quad (6)$$

The denominator in the above expression is:

$$s_{i,j} = \frac{\hat{\sigma}_\epsilon}{\sqrt{H_{i,j}}} \quad i, j = 1, \dots, k; i \neq j \quad (7)$$

The quantity  $H_{i,j}$  is the harmonic mean of the number of observations in columns  $i$  and  $j$ . The quantity  $\hat{\sigma}_\epsilon$  is the square root of the Mean Square Error determined in the one-way ANOVA procedure.

#### 4.7.3 Scheffe's method

The Scheffè's Test is a post-hoc test used in Analysis of Variance. Conducting ANOVA if the null hypothesis is rejected, that the means are the same, then Scheffe's test could be run to find out which pairs of means are significant. The Scheffe test corrects alpha for simple and



complex mean comparisons. Complex mean comparisons involve comparing more than one pair of means simultaneously. A statistic named T is defined as the ratio of unsigned contrast mean to contrast standard error, for Scheffe's method (ITL, 2007).

$$T_{i,j} = \frac{Q_{i,j}}{\sqrt{2}} \quad (8)$$

The Scheffè's 's method provides a formula which directly leads to the Scheffé p-value corresponding to an observed value of T as:

$$T = 1 - F\left(\frac{T^2}{k-1}, k-1, v\right) \quad (9)$$

Here, F() is the cumulative *F* distribution with its two degrees of freedom parameters *k*-1 and *v*. *k* is the number of treatments and *v* is the degrees of freedom of error. The Scheffé p-value of the observed T-statistic  $T_{i,j}$  is shown below for all relevant pairs of treatments Scheffé inference based on the p-value (ITL, 2007).

## CHAPTER

### 5 RESULTS AND DISCUSSION

#### 5.1 Data analysis

Voltage data were collected following the pre- and final experimental design procedures discussed in the previous chapter. These received data have been analyzed using statistical tools to identify which shape produces higher voltage comparing with other forms.

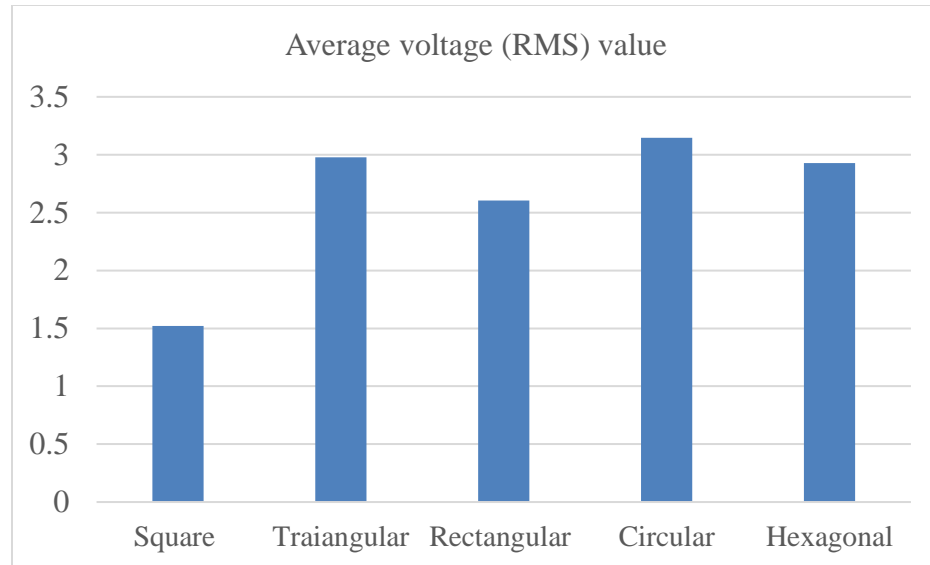
##### 5.1.1 Results of preliminary experimental design

Following the experimental procedure described in the previous chapter, 25 RMS voltage data were collected using oscilloscope from APA load wheel test. A table (Table 5) has been developed based on the average voltage (RMS) data produced by different shaped wafer-boxes coupled with PZT sensors. Table 5 also shows the ranking of varying wafer boxes according to the average voltage value.

**Table 5: Voltage (RMS volts) produced by different wafer box coupling with PZT sensors**

Sensor no	Square shape	Triangular shape	Rectangular shape	Circular shape	Hexagonal shape
<b>PZT Sensor 1</b>	1.694610	2.950110	2.761950	3.179740	2.852150
<b>PZT Sensor 2</b>	1.602920	2.941620	2.663300	3.196990	2.871570
<b>PZT Sensor 3</b>	1.478720	3.064040	2.584980	3.145170	2.971900
<b>PZT Sensor 4</b>	1.325400	3.024630	2.525710	3.090690	2.975150
<b>PZT Sensor 5</b>	1.502620	2.913280	2.484630	3.122080	2.967140
<b>Average</b>	1.520854	2.927582	2.604114	3.146934	2.978736
<b>Maximum</b>	1.694610	3.064040	2.761950	3.196990	2.975150
<b>Minimum</b>	1.325400	3.024630	2.484630	3.090690	2.967140
<b>Rank order</b>	5	3	4	1	2

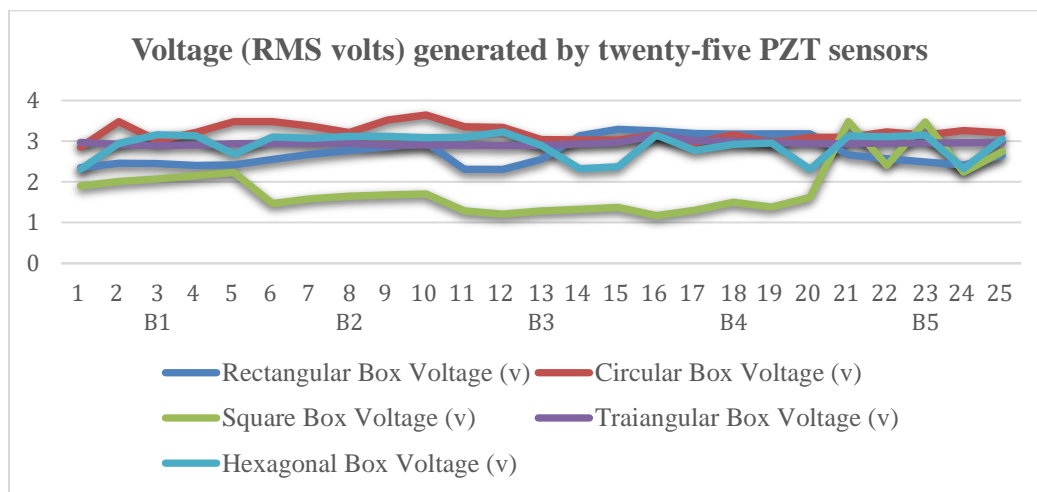
This figure 54 shows that the circularly shaped wafer box had the highest average voltage average than all other shapes. The hexagonal and triangular shaped boxes produced close voltage values. The square shape produced lowest level energy (voltage).



**Figure 54: Average voltage generated by different shaped wafer box**

### 5.1.2 Result of final experimental design

Table 6 shows the 125 voltage (RMS) values produced by twenty-five PZT sensors coupled with five different shaped wafer boxes. The sensors have been arranged according to their blocks.



**Figure 55: Voltage generated by PZT sensors for different shaped wafer box**

Figure 55 has been developed in Excel using the data from table 6. This figure shows that in majority of cases, the circularly shaped wafer box had the highest average voltage values compared to all other shapes. The square shaped box had the lowest average values of all shapes

tested. A detail statistical analysis has been conducted to determine if a significant difference exists between the different data groups and is discussed in a later part of this chapter

Table 6 shows the various average values produced by different PZT sensors embedded in the wafer-box. Here, it has also been displayed the ranking of varying wafer boxes according to the average voltage value.

**Table 6: Voltage (RMS volts) data generated by twenty-five PZT sensors embedded in different shaped Wafer-box under 152lbs. wheel load**

Group	Sensor no	Voltage (RMS volts) value produced by the different shape				
		Rectangular Box	Circular Box	Square box	Triangular Box	Hexagonal Box
B1	1	2.35069	2.85188	1.9028	2.96715	2.3093
	2	2.45843	3.48145	2.0067	2.92065	2.945
	3	2.45389	3.0158	2.07465	2.88828	3.1562
	4	2.40305	3.21455	2.14892	2.90882	3.13517
	5	2.41855	3.47637	2.2267	2.93443	2.68132
B2	6	2.55527	3.47673	1.47009	2.94454	3.10462
	7	2.68132	3.36679	1.58473	2.94399	3.0723
	8	2.76957	3.21578	1.65087	2.94598	3.11833
	9	2.86102	3.51812	1.67698	2.90115	3.11625
	10	2.96965	3.64371	1.7048	2.90574	3.08728
B3	11	2.30925	3.353	1.29077	2.89624	3.0912
	12	2.30624	3.33846	1.20859	2.89171	3.22762
	13	2.5561	3.03746	1.28922	2.89475	2.89475
	14	3.13517	3.03515	1.32674	2.93199	2.3267
	15	3.29134	3.02763	1.37448	2.97059	2.37448
B4	16	3.25516	3.16447	1.17228	3.13897	3.15207
	17	3.19318	2.96146	1.2989	3.0192	2.7696
	18	3.17023	3.15617	1.49626	2.99831	2.9207
	19	3.1834	2.96715	1.38222	2.96848	2.9513
	20	3.17928	3.09344	1.61977	2.93913	2.3093
B5	21	2.66515	3.09118	3.21247	2.94016	3.12783
	22	2.56721	3.22762	2.40297	2.9524	3.10776
	23	2.48994	3.15208	3.47403	2.95168	3.15211
	24	2.40907	3.25625	2.23919	2.96276	2.32766
	25	2.65109	3.20894	2.73877	2.96963	3.05189
<b>Average</b>		2.73133	3.2132656	1.849756	2.9474692	2.9004296
<b>Maximum</b>		3.02763	3.64371	3.21247	3.13897	3.22762
<b>Minimum</b>		2.30624	2.85188	1.9028	2.97615	2.3093
<b>Rank order</b>		4	1	5	2	3

## 5.2 Statistical analysis of voltage data generated by twenty-five PZT sensors

In this research project, a statistical tool ANOVA has been used to identify if significant difference lies within group sample voltage data. There was one independent variable (voltage) for all groups here. Thus, one-way ANOVA test was best suited for this research datasets. The ANOVA calculations for above datasets (Table 6) are given below.

### 5.2.1 One-way ANOVA analysis

**Table 7: Descriptive statistics for 5 class (5 shapes) independent treatments**

Treatment	C	H	S	R	T	Total
Observations N	25	25	25	25	25	125
sum $\sum x_i$	68.2832	80.3316	46.2439	73.6867	72.5107	341.056
Mean $\bar{x}$	2.7313	3.2133	1.8498	2.9475	212.724	973.753
the sum of squares $\sum x_i^2$	189.2661	259.106	95.4025	217.255	212.724	973.753
sample variance $s^2$	0.1151	0.0408	0.4109	0.0027	0.1005	0.3484
sample std. dev. $s$	0.3392	0.202	0.641	0.0521	0.317	0.5902
std. dev. of mean $SE_{\bar{x}}$	0.0678	0.0404	0.1282	0.0104	0.0634	0.0528

\*C = Circular shaped wafer box, \*S = Square shaped wafer box, \*H= Hexagonal shaped wafer box, \*R =Rectangular shaped wafer box, \*T = Triangular shaped wafer box

The total sample size is  $N = 125$ .

Therefore, the total degrees of freedom are:

$$df_{total} = 125 - 1 = 124$$

Also, the between-groups degrees of freedom are

$$df_{between} = 5 - 1 = 4,$$

The within-groups degrees of freedom are:

$$df_{within} = df_{total} - df_{between} = 124 - 4 = 120$$

It is needed to calculate the total sum of values and the grand mean. The following is obtained

$$\sum_{ij} X_{ij} = 68.28325 + 80.33164 + 46.2439 + 73.68673 + 72.51074 = 341.05626$$

The sum of squared values is

$$\sum_{ij} X_{ij}^2 = 189.2661 + 259.10583 + 95.40245 + 217.2546 + 212.7236 = 973.7526$$

The following total sum of squares was computed

$$SS_{total} = \sum_{ij} X_{ij}^2 - \frac{1}{N} (\sum_{IJ} X_{IJ})^2 = 973.7526 - \frac{341.05626^2}{125} = 42.456$$

The within the sum of squares is computed as shown in the calculation below:

$$SS_{within} = \sum SS_{withingroups} = 2.7620 + 0.9789 + 9.8625 + 0.0652 + 2.4113 = 16.08$$

Now that sum of squares is computed, we can proceed with computing the mean sum of squares:

$$MS_{between} = \frac{SS_{between}}{df_{between}} = \frac{42.456}{4} = 10.614$$

$$MS_{within} = \frac{SS_{within}}{df_{within}} = \frac{16.08}{124} = 0.134$$

Finally, with calculated the mean sum of squares, the F-statistic is computed as follows:

$$F = \frac{MS_{between}}{MS_{within}} = \frac{10.614}{0.134} = 79.21$$

### Null and Alternative Hypotheses

Null and alternative hypotheses were tested as follows:

$$H_0: \mu_1 = \mu_2 = \mu_3 = \mu_4 = \mu_5; \text{ all means are equal}$$

$$H_a: \text{Not all means are equal}$$

The above hypotheses were tested using an F-ratio for a One-Way ANOVA.

### Rejection Region

Based on the calculation, the significance level is  $\alpha = .05$ , and the degrees of freedom are  $df_1=4$  and  $df_2=4$ . Therefore, the rejection region for this F-test is  $R = \{F: F > F_c = 2.398\}$ .

And while, the significance level is  $\alpha = 0.01$ , and the degrees of freedom are  $df_1=4$  and  $df_2=4$ , therefore, the rejection region for this F-test is  $R = \{F: F > F_c = 3.48\}$

### Test Statistics

$$F = \frac{MS_{between}}{MS_{within}} = \frac{10.614}{0.134} = 79.21$$

### The decision about the null hypothesis

At significance level  $\alpha = .01$  it was observed that  $F = 79.21 > F_c = 2.398$ , it was then concluded that the null hypothesis was rejected. At  $\alpha = .05$  it was observed that  $F = 79.21 > F_c =$

3.48, it is then concluded that the null hypothesis was rejected. Using the P-value approach where  $p=0$  and  $p<0.05$ , the null hypothesis was rejected.

Data analysis determined that the null hypothesis proposed in this research study is not true. So, it can be claimed that not all 5 population means are equal both at significance level  $\alpha = 0.05$  and  $\alpha = 0.01$ . Here the p-value corresponding to the F-statistic of one-way ANOVA is lower than 0.01 which indicates that one or more pairs of treatments are significantly different.

### 5.2.2 Results of Tukey HSD Test

The critical value of the Tukey-Kramer HSD Q statistic was established based on the  $k = 5$  treatments and  $v = 120$  degrees of freedom for the error term and the significance level  $\alpha = 0.01$  and 0.05 (p-values) in the Studentized Range (Duke University, 1998). The critical values for Q, for  $\alpha$  of 0.01 and 0.05, as  $Q_{critical}^{\alpha=0.01,k=5,v=120} = 4.7084$  and  $Q_{critical}^{\alpha=0.05,k=5,v=120} = 3.9170$ , respectively.

**Table 8: Results of Tukey HSD Test for voltage data produced by twenty-five PZT sensors**

Treatments pair	Tukey HSD Q statistic	Tukey HSD p-value	Tukey HSD inference
<b>R vs C</b>	6.5827	0.0010053	Significant
<b>R vs S</b>	12.0414	0.0010053	Significant
<b>R vs T</b>	2.9522	0.2323125	Insignificant
<b>R vs H</b>	2.3097	00.4799530	Insignificant
<b>C vs S</b>	18.6241	0.0010053	Significant
<b>C vs T</b>	3.6305	0.0833045	Insignificant
<b>C vs H</b>	4.2730	0.0251203	Significant
<b>S vs T</b>	14.9936	0.0010053	Significant
<b>S vs H</b>	14.3511	0.0010053	Significant
<b>T vs H</b>	0.6425	0.8999947	Insignificant

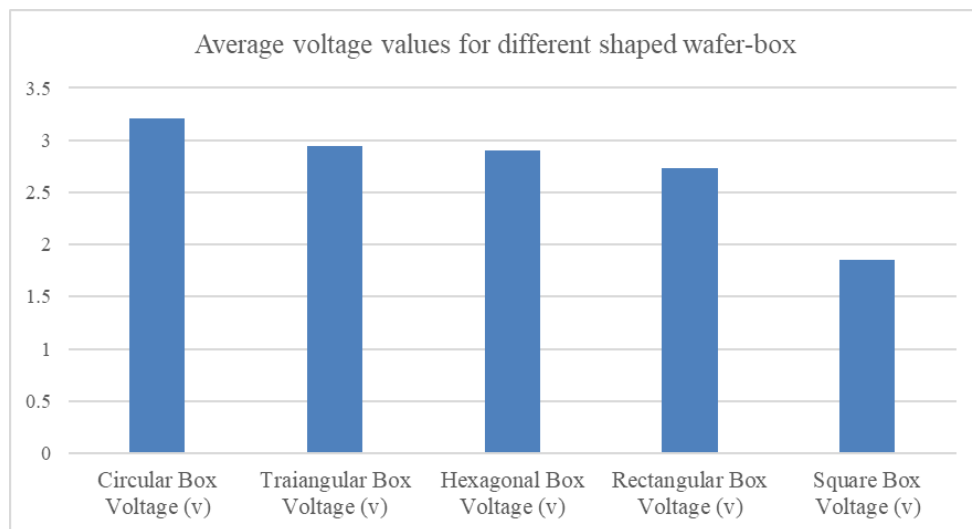
It can be identified from the Tukey HSD Test analysis above that there was a significant difference among different data groups. There were insignificant differences among rectangular, hexagonal and triangular voltage data groups at any confidence interval (significance level  $\alpha = 0.01$  and 0.05). The mean difference between circular and triangular shapes was also insignificant.

### 5.2.3 Results of Scheffe's method

It can also be identified from the statistical analysis in table 9 that there was a significant difference among different data sets. But it was seen that mean voltage difference among circular, triangular, square and hexagonal datasets were insignificant at any confidence interval (Significance level  $\alpha= 0.01$  and  $0.05$ ).

**Table 9: Results of Scheffe's method Test for voltage data produced by PZT sensor 1**

Treatments pair	Scheffé T-statistic	Scheffé p-value	Scheffé inference
R vs C	4.6547	0.0004814	Significant
R vs S	8.5145	1.1435e-11	Significant
R vs T	2.0875	0.3649261	Insignificant
R vs H	1.6332	0.6162234	Insignificant
C vs S	13.1692	1.1102e-16	Significant
C vs T	2.5672	0.1667754	Insignificant
C vs H	3.0215	0.0643987	Insignificant
S vs T	10.3021	2.2204e-16	Significant
S vs H	10.1478	2.1094e-15	Significant
T vs H	0.4543	0.9949553	Insignificant



**Figure 56: Average voltage (RMS volts) produced by twenty-five sensors embedded with different shaped wafer box**



A simple graph was designed using Microsoft Excel and is presented above (Figure 56). Each bar represents the average voltage value produced by twenty-five sensors embedded into different shaped wafer-boxes. From this graph it is easily seen that the circular shape has the highest average energy (voltage), and the square-shaped box produces lowest average voltage value.

A detail study of structural properties (section modulus, radius of gyration, area moment of inertia, extreme points) of wafer-box have been conducted in detail (Appendix A). A detail regression analysis has been conducted to determine which structural factor is most influential to produce electricity (Appendix A).

## CHAPTER

### 6 CONCLUSIONS AND RECOMMENDATIONS

#### 6.1 Conclusions

The primary research objective was to identify the shape effect of a wafer-box to produce energy while being coupled with PZT sensors. To be more specific it was defined which shape has the highest impact on energy harvesting higher voltage compared to the other forms of the same material.

The research framework was developed cautiously to achieve objective research results. The literature was studied to attain an impression of the essential aspects of the topic. It helped to prevent the repetition of errors occurring in previous research. Studying ASTM and UL standards were most important part of the literature review. These standards worked as supporting guidelines to obtain the research results.

The 3-D printers have ability to print wafer-box within very short period of time with high precision measurements. It can print any parts so cheap. The 3-D printer can print the product accurately which gives the more reliable output. Using the 3-D printer five different shaped wafer box were printed.

Experiments were designed in two stages. In the preliminary experiment five PZT sensors were randomly chosen to be used in a wafer-box to produce energy. In the final experiments, twenty-five PZT sensors were used with five boxes.

To accomplish the research objectives, multiple tests were conducted to identify which shape has the highest effect on harvesting energy. To produce energy, loaded wheel tests were run on an APA machine. The PZT sensors generated mechanical energy by APA wheel loads which was converted to electrical energy (voltage) by using an electronic rectifier. The rectifier received AC voltage from the PZT sensors and converted the AC voltage to DC output. Next the oscilloscope received the DC voltage from rectifier displaying the DC voltage as RMS volts.

To analyze the acquired voltage data, descriptive statistics, an ANOVA test, a Tukey HSD test, and a Scheffe's test methods were conducted.

The test results for both the preliminary and final experiments indicated that the circular shape produced the highest positive effect on energy harvesting compared with other shapes. The triangular shape occupied the second position. In the final experiment the average voltage production by circular and triangular shape were 3.2132 volts and 2.9474 volts respectively. The square shaped box was in the lowest place to harvest energy. In the final experiment the average voltage produced by the square shape was 1.8497 volts.

The achieved result can be used as a knowledge base for different government agencies or private industry working with newly-developed and advanced piezoelectric technologies.

## **6.2 Recommendations and limitations**

It is recommended to maintain uniformity of test environment for all experiments to obtain identical outputs. While conducting a preliminary experiment, the channel 1 port of oscilloscope was used to collect RMS voltage value generated by PZT sensors from APA load wheel tests. But the channel 1 did not properly respond. The channel did not display the correct output. Then channel 4 port was used to obtain voltage data from APA load wheel tests. The same channel was used for the final experiment to maintain the stable condition for both preliminary and final experiments.

Same test conditions were applied for both experiments. For both experiments wheel load was set to 152lbs. The test speed was set at 30Hz and APA temperature was set 30 degrees Celsius for both experiments. It was necessary to maintain uniform test conditions to receive identical output from both experiments. If the test conditions are same, it is possible to compare outputs of all experiments.

The wafer-box coupled with PZT sensors must be static on APA ground so that the box cannot move from its place when wheel loads are applied. The load wheel must run freely on the wafer box. If these conditions are not maintained output will be affected by extraneous variables. Same rules are also applicable for PZT sensors while being embedded into wafer-box otherwise the result would be different.

The Lulzbot TAZ 6 3D-printer can print materials using more strong materials like wood, aluminum and steel. In this research project high strength material filament was not used due to their high cost and a budget issue. This research knowledge could be used as a standard method

of energy harvesting technology. This research method could be applied to other 3-D printed materials to identify their contribution to energy harvesting.

## REFERENCES

(2018, April). Retrieved from Engineers Edge:

[https://www.engineersedge.com/calculators/section\\_square\\_case\\_11.htm](https://www.engineersedge.com/calculators/section_square_case_11.htm)

Alperen Topra, O. T. (2014). Piezoelectric energy harvesting: State-of-the-art and challenges. *American Institute of Physics*.

Ang Hu, Y. F.-J. (1999). Humidity Dependence of Apparent Dielectric Constant for DSP Cement Materials at High Frequencies. *Journal of the American Ceramic Society*.

APC International. (2018). *APC International*. Retrieved from <https://www.americanpiezo.com>:  
<https://www.americanpiezo.com/piezo-theory/pzt.html>

ASTM C 42/C 42M – 03. (2003). Standard Test Method for Obtaining and Testing Drilled Cores and Sawed Beams of Concrete. 100 Barr Harbor Drive, PO Box C700, West Conshohocken, PA 19428-2959, United States: ASTM International.

ASTM C 496/C 496M. (2004). Standard Test Method for Splitting Tensile Strength of Cylindrical Concrete Specimens. *C 496/C 496M – 04*. 100 Barr Harbor Drive, PO Box C700, West Conshohocken, PA 19428-2959, United States: ASTM International.

ASTM C 78 . (2002). *ASTM C 78 – 02. Standard Test Method for Flexural Strength of Concrete (Using Simple Beam with Third-Point Loading)*. 100 Barr Harbor Drive, PO Box C700, West Conshohocken, PA 19428-2959, United States: ASTM International.

ASTM D 618. (2000). *ASTM D 618 – 00. Standard Practice for Conditioning Plastics for Testing*. 100 Barr Harbor Drive, PO Box C700, West Conshohocken, PA 19428-2959, United States: ASTM International.

ASTM D 638. (2002). *ASTM D 638 - 02a. Standard Test Method for Tensile Properties of Plastics*. 100 Barr Harbor Drive, PO Box C700, West Conshohocken, PA 19428-2959, United States.: ASTM International.

ASTM E650. (1997). *ASTM E650 - 97. Standard Guide for Mounting Piezoelectric Acoustic Emission Sensors*. 100 Barr Harbor Drive, West Conshohocken, PA 19428-2959, United States: ASTM International.

- ASTM International. (2000). *Standardization News*. Retrieved from [https://www.astm.org/SNEWS/OCTOBER\\_2000/oct\\_howto.html](https://www.astm.org/SNEWS/OCTOBER_2000/oct_howto.html)
- ASTM International. (2003). C 39/C 39M – 03. *Standard Test Method for Compressive Strength of Cylindrical Concrete Specimens*. 100 Barr Harbor Drive, PO Box C700, West Conshohocken, PA 19428-2959, United States: ASTM International.
- ASTM International. (2006). Standard Test Method for Density, Absorption, and Voids in Hardened Concrete. *C 642-06*. 100 Barr Harbor Drive, PO Box C700, West Conshohocken, PA 19428-2959, United States: ASTM International.
- ASTM International. (2018). *ASTM International*. Retrieved from <https://www.astm.org/>
- Basari et al., e. a. (2014). Shape Effect of Piezoelectric Energy Harvester on Vibration Power Generation. *Journal of Power and Energy Engineering*, 8.
- C. Keawboonchuay, T. G. (2003). Maximum Power Generation in a Piezoelectric Pulse Generator. *IEEE Transactions on Plasma Science*.
- CIRT. (2018). *Types of Experimental Research*. Retrieved from Center for Innovation in Research and Teaching: [https://cirt.gcu.edu/research/developmentresources/research\\_ready/experimental/design\\_types](https://cirt.gcu.edu/research/developmentresources/research_ready/experimental/design_types)
- Duke University. (1998). Studentized Range distribution. *The studentized range statistic*. Duke University.
- Engineers Edge*. (2018, April). Retrieved from [https://www.engineersedge.com/calculators/section\\_square\\_case\\_6.htm](https://www.engineersedge.com/calculators/section_square_case_6.htm)
- Engineers Edge*. (2018, April). Retrieved from [https://www.engineersedge.com/calculators/section\\_square\\_case\\_15.htm](https://www.engineersedge.com/calculators/section_square_case_15.htm)
- Engineers Edge*. (2018, April). Retrieved from [https://www.engineersedge.com/calculators/section\\_square\\_case\\_15.htm](https://www.engineersedge.com/calculators/section_square_case_15.htm)
- ITL. (2007). <http://www.itl.nist.gov>. Retrieved from National Institute of Standards and Technology: <http://www.itl.nist.gov/div898/handbook/prc/section4/prc471.htm>

- ITL. (2007). *National Institute of Standards and Technology*. Retrieved from NIST:  
<http://www.itl.nist.gov/div898/handbook/prc/section4/prc472.htm>
- Kaur et al., e. a. (2016). Effect of Various Shapes and Materials on the Generated Power for Piezoelectric Energy Harvesting System. *American Institute of Physics*.
- Kim et al. (2011). A review of piezoelectric energy harvesting based on vibration. *International Journal of Precision Engineering and Manufacturing*, 7.  
doi:<https://doi.org/10.1007/s12541-011-0151-3>
- Kim et al., e. a. (2018). Energy Harvesting Assessment Using PZT Sensors and Roadway Materials. *Annual TRB Conference*. Washington: TRB.
- Lind D., M. W. (2015). *Statistical Techniques in Business and Economics*. New York: McGraw-Hill Education.
- Macromatic Inc. (2018). *Macromatic*. Retrieved from Macromatic Industrial Controls, Inc:  
<https://www.macromatic.com/blog/relays/what-is-true-rms-and-why-is-it-important-in-a-phase-monitor>
- Mane et al., e. a. (2012). Studying the effects of temperature on energy harvesting using pre-stressed piezoelectric diaphragms. *NASA Langley Research Center*, 11.
- Pasha, Z. B. (2016). Effect of temperature and loading on output voltage of lead. *IOP Science*.
- RAE. (2018). *Royal Academy of Engineering*. Retrieved from  
<https://www.raeng.org.uk/publications/other/8-rms>
- Sihai Wen, D. (2002). Piezoelectric cement-based materials with large coupling and voltage coefficients. *Cement and Concrete Research, ELSEVIER*, 5.
- Six Sigma. (2016). *SAS-Concepts of Experimental Design*.  
<https://support.sas.com/resources/papers/sixsigma1.pdf>.
- UL 1077. (2015). *Standard for Supplementary Protectors for Use in Electrical Equipment*. Underwriters Laboratories.
- UL 1805. (2002, 06 07). UL 1805. *Standard for Laboratory Hoods and Cabinets*. UL.

- UL 61010-1. (2016, 04 29). UL 61010-1. *Safety Requirements for Electrical Equipment for Measurement, Control, and Laboratory Use*. UL.
- UL 61010-2-12. (2017, 02 20). UL 61010-2-12. *Standard for Safety Requirements for Electrical Equipment for Measurement, Control and Laboratory Use - Part 2-012: Particular Requirements for Climatic and Environmental Testing and Other Temperature Conditioning Equipment*. UL.
- UL 61010-2-30 . (16, 09 2016). UL 61010-2-30 . *Safety requirements for electrical equipment for measurement, control, and laboratory use - Part 2-030: Particular requirements for testing and measuring circuits*. UL.
- UL 61010-2-33. (2014, 08 08). UL 61010-2-33. *Standard for Safety Requirements for Electrical Equipment for Measurement, Control, and Laboratory Use - Part 2-033: Particular Requirements for Hand-Held Multimeters and Other Meters, for Domestic and Professional Use, Capable of Measuring Mains V*.
- UL INC. (2015). *Style Manual for UL Standards for Saffaety*. Uderwriter Laboratories Inc.
- UMass Amherst Libraries . (2017, Aug 08). *UMass Amherst Libraries* . Retrieved from Types of ASTM Standards: <http://guides.library.umass.edu/c.php?g=672684&p=4736812>
- Wikipedia. (2016, May). *Random assignment*. Retrieved from Wikipedia:  
[https://en.wikipedia.org/wiki/Random\\_assignment](https://en.wikipedia.org/wiki/Random_assignment)
- Wikipedia. (2018). *Section Modulus*. Retrieved from Wikipedia The Free Encyclopedia:  
[https://en.wikipedia.org/wiki/Section\\_modulus](https://en.wikipedia.org/wiki/Section_modulus)
- Yale University. (1997). *Department of Statistics and Data Science*. Retrieved from Experimentation: <http://www.stat.yale.edu/Courses/1997-98/101/expdes.htm>



## APPENDIX A

### Section modulus

Section modulus is the cross-sectional geometric property of structural members. This property is used to design beams and flexural members (Wikipedia, 2018). Radius of gyration, moment of inertia, polar moment of inertia, area for tension and shear are some other properties used in the design process. Structural shape has great impact on relationship among these properties.

If the section modulus is high the member is more resistant to bending moment of the beam. When two plates of same materials are compared according to their section modulus value the plate having higher section modulus can bear higher loads than the plate with lower section modulus (Wikipedia, 2018). Section modulus calculation formula for different shape and the calculated results have been given below:

#### 1. Section modulus calculation: Circle

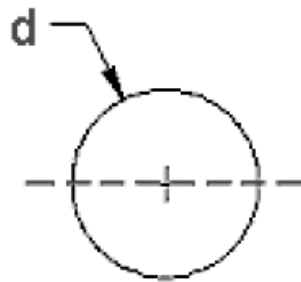


Figure 57: Circular shape

Table 10: Section modulus calculation equations for circular shape (Engineers Edge, 2018)

Description	Equation
Area moment of inertia section properties = I	$\pi d^4/64$
<b>Section Modulus Z = I/y</b>	<b><math>\pi d^3/32</math></b>
Radius of gyration	d/4
y = distance from axis to extreme fiber	d/2

## 2. Section modulus calculation: Triangle

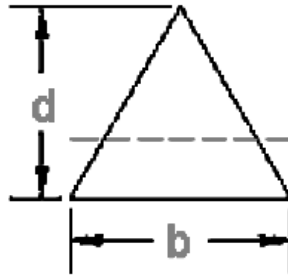


Figure 58: Triangular shape

Table 11: Section modulus calculation equations for triangular shape (*Engineers Edge, 2018*)

Description	Equation
Area moment of inertia section properties = I	$\pi d^3/36$
<b>Section Modulus <math>Z = I/y</math></b>	<b><math>bd^2/24</math></b>
Radius of gyration	$d/\sqrt{18}$
y = distance from axis to extreme fiber	$2d/3$

## 3. Section modulus calculation: Hexagon

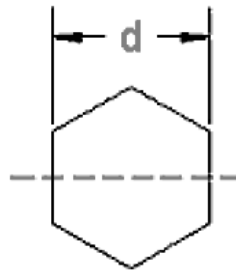


Figure 59: Hexagonal shape

Table 12: Section modulus calculation equations for hexagonal shape (*Engineers Edge, 2018*)

Description	Equation
Area moment of inertia section properties = I	$\frac{A}{12} \left[ \frac{d^2(1 + 2 \cos^2 30^\circ)}{4 \cos^2 30^\circ} \right]$
<b>Section Modulus <math>Z = \frac{I}{y}</math></b>	<b><math>\frac{A}{6.9} \left[ \frac{d^2(1 + 2 \cos^2 30^\circ)}{4 \cos^2 30^\circ} \right]</math></b>

Radius of gyration	$\sqrt{\frac{d^2(1 + 2 \cos^2 30^\circ)}{48 \cos^2 30^\circ}}$
y = distance from axis to extreme fiber	$\frac{d}{2 \cos 30^\circ}$

#### 4. Section modulus calculation: Rectangle

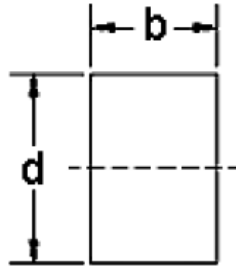


Figure 60: Rectangular shape

Table 13: Section modulus calculation equations for rectangular shape (*Engineers Edge, 2018*)

Description	Equation
Area moment of inertia section properties = I	$bd^3/12$
<b>Section Modulus Z = I/y</b>	<b><math>bd^2/6</math></b>
Radius of gyration	$d/\sqrt{12}$
y = distance from axis to extreme fiber	$d/2$

#### 5. Section modulus calculation: Square

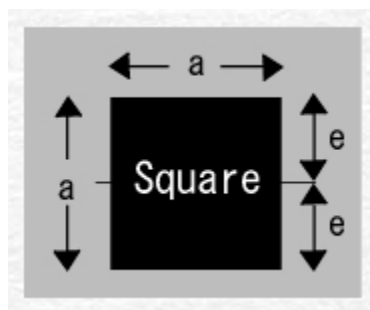


Figure 61: Square shape

**Table 14: Section modulus calculation equations for square shape** (*Engineers Edge, 2018*)

Description	Equation
Area moment of inertia section properties = I	$a^4/12$
<b>Section Modulus <math>Z = I/y</math></b>	<b><math>a^3/6</math></b>
Radius of gyration	$4/\sqrt{12}$
y = distance from axis to extreme fiber	a/2

The structural property values have been given in the following table. These values have been calculated using the above equations.

**Table 15: Section modulus calculation for five different shapes**

Descriptions	Values				
	Circular	Triangular	Hexagonal	Rectangular	Square
Area Moment of Inertia Section Properties (inch <sup>4</sup> )	139.15138	239.2961	202.81994	142.41983	205.7792
Section modulus (inch <sup>3</sup> )	<b>38.12367</b>	<b>38.59616</b>	<b>46.10552</b>	<b>48.71977</b>	<b>58.41512</b>
Radius of gyration (inch)	1.825	2.1948	2.013	1.69065	2.03745
Extreme points (inch)	3.65	6.2	4.39962	2.925	3.525

From the table 15 it can be identified that square shape had the lowest section modulus and square shape had the highest section modulus. So, it can be assumed that the circular shaped wafer-box is less resistant to bending moment and square shape is highest resistant. The triangular, hexagonal and rectangular shaped occupied the second, third and fourth place respectively according to their section modulus values.

Thus, lower the section modulus the wafer-box will bend more when force is applied to it. The wafer-box with higher section modulus will bend less. Out of five shapes circular shaped box wafer box will bend more than other shapes. The square box will bend lowest as it has the highest section modulus value.

As circular box bended more due to the lower section modulus the PZT sensors were bended more as well. More the PZT sensors bended more electricity was produced. According to this principle the square shape produced the lowest energy as it bended least due to its highest section modulus property. The energy production by other three shapes (triangular, square, rectangular) could be illustrated by this bending moment principle.

## Calculation of linear regression

### Regression analysis using section modulus and average voltage value

For this calculation the section modulus is take as independent variable and average voltage value is the dependent variable. The linear regression is calculated based on following entries:

**Table 16: Section modulus and average voltage value table**

Axis label	Values				
	Circular shape	Triangular shape	Hexagonal shape	Rectangular shape	Square shape
<b>X (Section modulus)</b>	38.12367	38.59616	46.10552	48.71977	58.41512
<b>Y (Average voltage)</b>	3.2132656	2.9474692	2.9004296	2.73133	1.849756

The equation of linear regression is:

$$y = a + bx$$

Step 1: At first it was calculated  $XY$  and  $X^2$

**Table 17: Linear fit-curve calculation**

<b>X</b>	<b>Y</b>	<b>XY</b>	<b>X<sup>2</sup></b>
38.12367	3.2132656	122.501477357	1483.41421427
38.59616	2.9474692	113.760992838	1489.66356675
46.10552	2.9004296	133.725814931	2125.71897447
48.71977	2.73133	133.069769394	2373.61598885
58.41512	1.849756	108.053718711	3412.32624461

Step 2: Then it was calculated sum of each column:

$$\sum X = 229.96024$$

$$\sum Y = 13.6422504$$

$$\sum XY = 611.111773231$$

$$\sum X^2 = 10854.738989$$

Step 3: The it was calculated the value of  $a$  and  $b$  using following equations:

$$a = \frac{\sum Y \sum X^2 - \sum X \sum XY}{n \sum X^2 - (\sum X)^2} = \frac{13.6422504 \cdot 10854.738989 - 229.96024 \cdot 611.111773231}{5 \cdot 10854.738989 - 229.96024^2} = 5.425$$

$$b = \frac{n \sum XY - \sum X \sum Y}{n \sum X^2 - (\sum X)^2} = \frac{5 \cdot 611.111773231 - 229.96024 \cdot 13.6422504}{5 \cdot 10854.738989 - 229.96024^2} = -0.059$$

Step 4: The value of a and b is substituted in linear equation formula (1)

$$y = a + bx$$

$$y = 5.425 - 0.059x$$

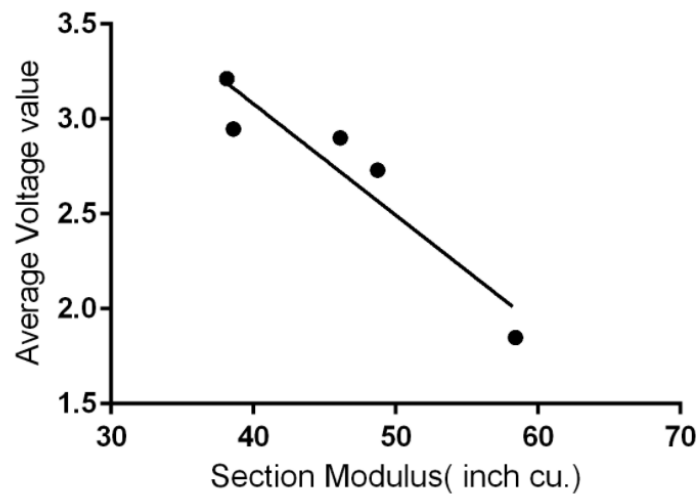
The equation of co-efficient of correlation is calculated using following equation:

$$r = \frac{n \sum XY - \sum X \sum Y}{\sqrt{[n \sum X^2 - (\sum X)^2][n \sum Y^2 - (\sum Y)^2]}}$$

The calculated co-efficient of correlation is

$$r = -0.9393$$

Negative value means there is negative relationship between section modulus and voltage production.



**Figure 62: Linear regression fit-curve for section modulus and average voltage value**

The calculated  $R^2$  value is 0.8823 which is close to 1 which means the regression model fits the observations better condition. The section modulus and average voltage production have strongly negative relationship. So, it can be said if section modulus increased the voltage production by wafer-box will decrease and vice-versa.

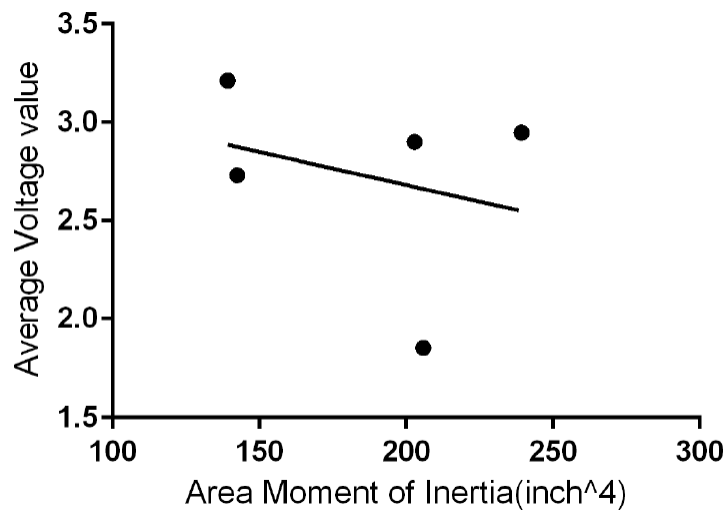
### Regression analysis using area moment of inertia and average voltage value

**Table 18:: Area moment of inertia and average voltage value table**

Axis label	Values				
	Circular shape	Triangular shape	Hexagonal shape	Rectangular shape	Square shape
<b>X (Area moment of inertia)</b>	139.15138	239.2961	202.81994	142.41983	205.7792
<b>Y (Average voltage)</b>	3.2132656	2.9474692	2.9004296	2.73133	1.849756

The calculate regression line is:

$$y = 3.355 - 0.003x$$



**Figure 63:Linear regression fit-curve for area moment of inertia and average voltage value**

The calculated  $r$  value is:

$$r = -0.2824$$

The calculated  $R^2$  value is

$$R^2 = 0.08$$

$r$  value is negative which means there is negative relationship between area moment of inertia and average voltage. So, when area moment of inertia increases voltage the value decreases. But the  $R^2$  value is 0.08 which is means this relationship is very weak.

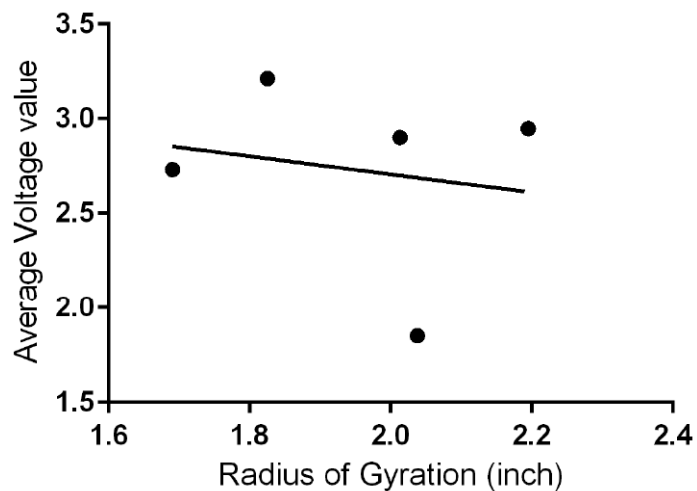
### Regression analysis using radius of gyration and average voltage value

**Table 19: Radius of gyration and average voltage value table**

Axis label	Values				
	Circular shape	Triangular shape	Hexagonal shape	Rectangular shape	Square shape
<i>X</i> (Radius of gyration)	1.825	2.1948	2.013	1.69065	2.03745
<i>Y</i> (Average voltage)	3.2132656	2.9474692	2.9004296	2.73133	1.849756

The calculated regression line is:

$$y = 3.3661 - 0.478x$$



**Figure 64: Linear regression fit-curve for radius of gyration and average voltage value**

The calculated  $r$  value is:

$$r = -0.1802$$

The calculated  $R^2$  value is

$$R^2 = 0.033$$

$r$  value is negative which means there is negative relationship between radius of gyration and average voltage. So, when radius of gyration value increases the voltage value decreases and vice-versa. But the  $R^2$  value is 0.033 which means this relationship is very weak.



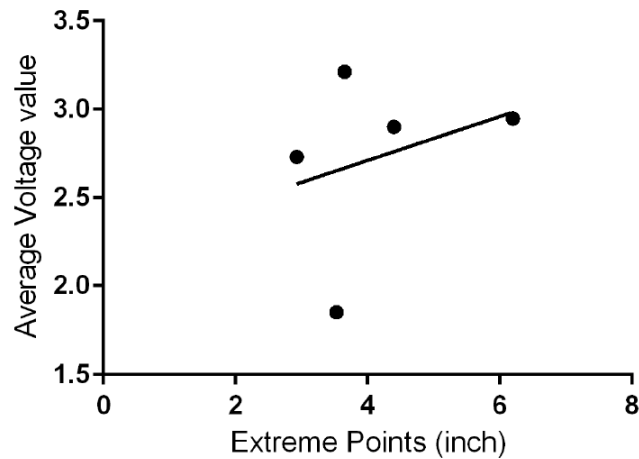
### Regression analysis using extreme points and average voltage value

**Table 20: Extreme points and average voltage value table**

Axis label	Values				
	Circular shape	Triangular shape	Hexagonal shape	Rectangular shape	Square shape
X (Extreme points)	3.65	6.2	4.39962	2.925	3.525
Y (Average voltage)	3.2132656	2.9474692	2.9004296	2.73133	1.849756

The calculate regression line is:

$$y = 2.215 + 0.124x$$



**Figure 65: Linear regression fit-curve for extreme points and average voltage value**

The calculated  $r$  value is:

$$r = 0.3017$$

The calculated  $R^2$  value is

$$R^2 = 0.091$$

$r$  value is positive which means there is positive relationship between extreme points and average voltage. So, when area extreme point value increases the voltage value also increases.

But the  $R^2$  value is 0.091 which is means this relationship is very weak.

**Table 21: Summary of regression calculation with structural properties and average voltage data**

Regression status	Relation analysis with average voltage value of 125 voltage data and different structural properties of wafer box			
	Area moment of inertia and	Section modulus	Radius of gyration	Extreme points
$r$	-0.2824	-0.9393	-0.1802	0.3017
$R^2$	0.08	0.8823	0.033	0.091
<b>Relationship</b>	Very weak negative relationship	<b>Very strong negative relationship</b>	Very weak negative relationship	Very weak positive relationship
<b>Independent and dependent variable relationship significance</b>	Insignificant	<b>Significant</b>	Insignificant	Insignificant

### Summary analysis

The  $R^2$  value for area moment of inertia is 0.08. This value means area moment of inertia explains an estimated 8% of the variation in average voltage data. The  $R^2$  value for radius of gyration and extreme points are 0.033 and 0.091 respectively. This indicates radius of gyration explains 3.3% of variation in average voltage data and extreme point explains 9.1%. The  $R^2$  value for section value is 0.8823. This means this section modulus can occur 88.23% variation in average voltage values. Thus, from regression analysis it could be said, out of four properties the section value is the most influential structural properties to alter voltage production.

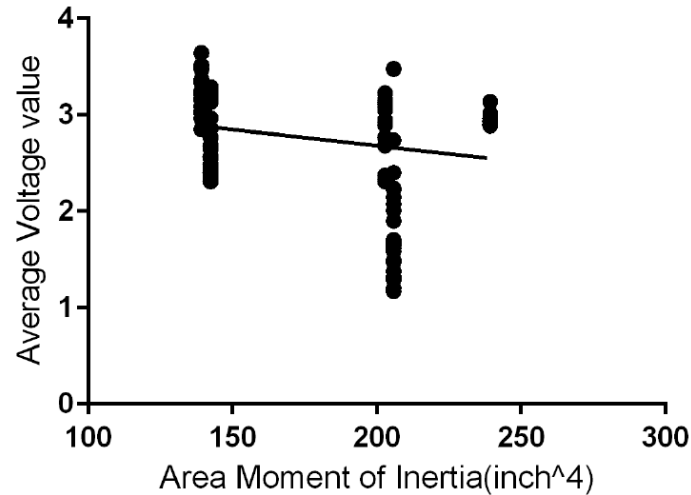
### Regression analysis using different structural properties and 125 voltage values

The data values used to compute regression values using different structural properties (section modulus, radius of gyration, extreme points, area moment of inertia area moment of inertia) and 125 voltage values have been shown in table 23.

### Regression analysis using are moment of inertia and 125 voltage values

The calculated regression line is:

$$y = 3.355 - 0.003x$$



**Figure 66: Linear regression fit-curve for area moment of inertia and 125 voltage value**

The calculated  $r$  value is:

$$r = -0.2237$$

The calculated  $R^2$  value is

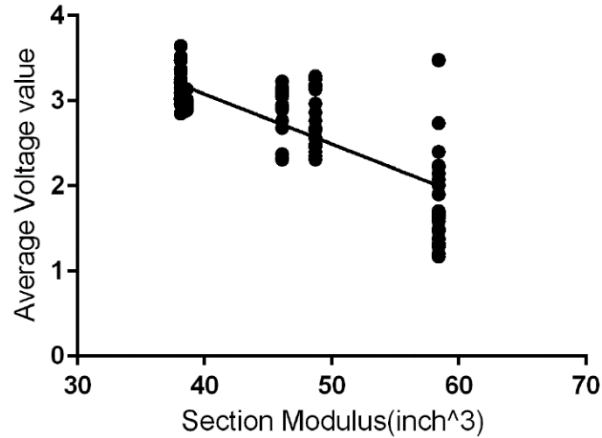
$$R^2 = 0.05005$$

$r$  value is negative which means there is negative relationship between area moment of inertia and average voltage. So, when area moment of inertia increases the voltage value decreases and vice versa. But the  $R^2$  value is 0.05005 which is means this relationship is very weak.

### Regression analysis using are section modulus and 125 voltage values

The calculated regression line is:

$$y = 5.425 - 0.05863x$$



**Figure 67: Linear regression fit-curve for section modulus and 125 voltage value**

The calculated  $r$  value is:

$$r = -0.7442$$

The calculated  $R^2$  value is

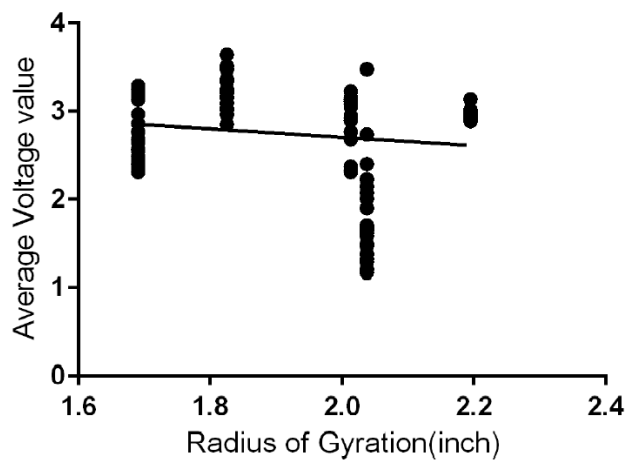
$$R^2 = 0.5539$$

$r$  value is negative which means there is negative relationship between area section modulus and average voltage. So, when area section modulus value increases the voltage value decreases and vice versa. But the  $R^2$  value is 0.5539 which means this relationship is strong.

### Regression analysis using are radius of gyration and 125 voltage values

The calculated regression line is:

$$y = 3.661 - 0.478x$$



**Figure 68: Linear regression fit-curve for radius of gyration and 125 voltage value**

The calculated  $r$  value is:

$$r = -0.1428$$

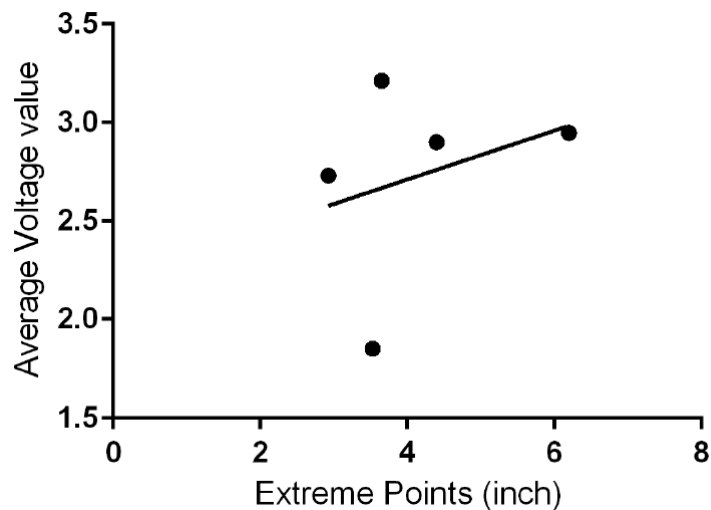
The calculated  $R^2$  value is

$$R^2 = 0.02038$$

### Regression analysis using are extreme point and 125 voltage values

The calculated regression line is:

$$y = 2.215 - 0.124x$$



**Figure 69: Linear regression fit-curve for extreme points and 125 voltage value**

The calculated  $r$  value is:

$$r = 0.239$$

The calculated  $R^2$  value is

$$R^2 = 0.05713$$

$r$  value is positive which means there is positive relationship between area moment of inertia and average voltage. So, when area moment of inertia increases voltage value also increases and vice-versa. But the  $R^2$  value is 0.08 which is means this relationship is very weak.

**Table 22: Summary of regression calculation with structural properties and 125 voltage data**

Regression status	Relation analysis with 125 voltage data (dependent variable) and different structural properties of wafer box (independent variable)			
	Area moment of Inertia and	Section modulus	Radius of Gyration	Extreme points
$r$	-0.2237	-0.7442	-0.1428	0.239
$R^2$	0.05005	0.5539	0.02038	0.05713
<b>Relationship</b>	Very weak negative relationship	<b>Moderately strong negative relationship</b>	Very weak negative relationship	Very weak positive relationship
<b>Independent and dependent variable relationship significance</b>	Insignificant	<b>Significant</b>	Insignificant	Insignificant

### Summary analysis

The  $R^2$  value for area moment of inertia is 0.05005. This value means area moment of inertia explains an estimated 5% of the variation in average voltage data. The  $R^2$  value for radius of gyration and extreme points are 0.02038 and 0.05713 respectively. This indicates radius of gyration explains 2.03% of variation in average voltage data and extreme point explains 5.71%. The  $R^2$  value for section value is 0.5539. This means this section modulus can occur 55.39% variation in average voltage values. Thus, from regression analysis it could be said, out of four properties the section most has most influential on voltage production.

**Table 23: 125 voltage data and structural property value table**

Y axis values (Dependent variable)	X axis values (Independent variable)			
Rectangular box voltage (v)	Are moment of inertia ( $inch^4$ )	Radius of gyration (inch)	Extreme points (inch)	Section modulus (cu. inch)
2.35069	142.41983	1.69065	2.925	48.71977

2.45843	142.41983	1.69065	2.925	48.71977
2.45389	142.41983	1.69065	2.925	48.71977
2.40305	142.41983	1.69065	2.925	48.71977
2.41855	142.41983	1.69065	2.925	48.71977
2.55527	142.41983	1.69065	2.925	48.71977
2.68132	142.41983	1.69065	2.925	48.71977
2.76957	142.41983	1.69065	2.925	48.71977
2.86102	142.41983	1.69065	2.925	48.71977
2.96965	142.41983	1.69065	2.925	48.71977
2.30925	142.41983	1.69065	2.925	48.71977
2.30624	142.41983	1.69065	2.925	48.71977
2.5561	142.41983	1.69065	2.925	48.71977
3.13517	142.41983	1.69065	2.925	48.71977
3.29134	142.41983	1.69065	2.925	48.71977
3.25516	142.41983	1.69065	2.925	48.71977
3.19318	142.41983	1.69065	2.925	48.71977
3.17023	142.41983	1.69065	2.925	48.71977
3.1834	142.41983	1.69065	2.925	48.71977
3.17928	142.41983	1.69065	2.925	48.71977
2.66515	142.41983	1.69065	2.925	48.71977
2.56721	142.41983	1.69065	2.925	48.71977
2.48994	142.41983	1.69065	2.925	48.71977
2.40907	142.41983	1.69065	2.925	48.71977
2.65109	142.41983	1.69065	2.925	48.71977
<b>Circular box voltage</b>				
2.85188	139.15138	1.825	3.65	38.12367
3.48145	139.15138	1.825	3.65	38.12367
3.0158	139.15138	1.825	3.65	38.12367
3.21455	139.15138	1.825	3.65	38.12367
3.47637	139.15138	1.825	3.65	38.12367
3.47673	139.15138	1.825	3.65	38.12367
3.36679	139.15138	1.825	3.65	38.12367
3.21578	139.15138	1.825	3.65	38.12367
3.51812	139.15138	1.825	3.65	38.12367
3.64371	139.15138	1.825	3.65	38.12367
3.353	139.15138	1.825	3.65	38.12367
3.33846	139.15138	1.825	3.65	38.12367
3.03746	139.15138	1.825	3.65	38.12367
3.03515	139.15138	1.825	3.65	38.12367
3.02763	139.15138	1.825	3.65	38.12367
3.16447	139.15138	1.825	3.65	38.12367
2.96146	139.15138	1.825	3.65	38.12367
3.15617	139.15138	1.825	3.65	38.12367

2.96715	139.15138	1.825	3.65	38.12367
3.09344	139.15138	1.825	3.65	38.12367
3.09118	139.15138	1.825	3.65	38.12367
3.22762	139.15138	1.825	3.65	38.12367
3.15208	139.15138	1.825	3.65	38.12367
3.25625	139.15138	1.825	3.65	38.12367
3.20894	139.15138	1.825	3.65	38.12367
<b>Square box voltage</b>				
1.9028	205.7792	2.03745	3.525	58.41512
2.0067	205.7792	2.03745	3.525	58.41512
2.07465	205.7792	2.03745	3.525	58.41512
2.14892	205.7792	2.03745	3.525	58.41512
2.2267	205.7792	2.03745	3.525	58.41512
1.47009	205.7792	2.03745	3.525	58.41512
1.58473	205.7792	2.03745	3.525	58.41512
1.65087	205.7792	2.03745	3.525	58.41512
1.67698	205.7792	2.03745	3.525	58.41512
1.7048	205.7792	2.03745	3.525	58.41512
1.29077	205.7792	2.03745	3.525	58.41512
1.20859	205.7792	2.03745	3.525	58.41512
1.28922	205.7792	2.03745	3.525	58.41512
1.32674	205.7792	2.03745	3.525	58.41512
1.37448	205.7792	2.03745	3.525	58.41512
1.17228	205.7792	2.03745	3.525	58.41512
1.2989	205.7792	2.03745	3.525	58.41512
1.49626	205.7792	2.03745	3.525	58.41512
1.38222	205.7792	2.03745	3.525	58.41512
1.61977	205.7792	2.03745	3.525	58.41512
3.48247	205.7792	2.03745	3.525	58.41512
2.40297	205.7792	2.03745	3.525	58.41512
3.47403	205.7792	2.03745	3.525	58.41512
2.23919	205.7792	2.03745	3.525	58.41512
2.73877	205.7792	2.03745	3.525	58.41512
<b>Triangular box voltage</b>				
2.96715	239.2961	2.1948	6.2	38.59616
2.92065	239.2961	2.1948	6.2	38.59616
2.88828	239.2961	2.1948	6.2	38.59616
2.90882	239.2961	2.1948	6.2	38.59616
2.93443	239.2961	2.1948	6.2	38.59616
2.94454	239.2961	2.1948	6.2	38.59616
2.94399	239.2961	2.1948	6.2	38.59616



2.94598	239.2961	2.1948	6.2	38.59616
2.90115	239.2961	2.1948	6.2	38.59616
2.90574	239.2961	2.1948	6.2	38.59616
2.89624	239.2961	2.1948	6.2	38.59616
2.89171	239.2961	2.1948	6.2	38.59616
2.89475	239.2961	2.1948	6.2	38.59616
2.93199	239.2961	2.1948	6.2	38.59616
2.97059	239.2961	2.1948	6.2	38.59616
3.13897	239.2961	2.1948	6.2	38.59616
3.0192	239.2961	2.1948	6.2	38.59616
2.99831	239.2961	2.1948	6.2	38.59616
2.96848	239.2961	2.1948	6.2	38.59616
2.93913	239.2961	2.1948	6.2	38.59616
2.94016	239.2961	2.1948	6.2	38.59616
2.9524	239.2961	2.1948	6.2	38.59616
2.95168	239.2961	2.1948	6.2	38.59616
2.96276	239.2961	2.1948	6.2	38.59616
2.96963	239.2961	2.1948	6.2	38.59616
<b>Hexagonal box voltage</b>				
2.3093	202.81994	2.013	4.39962	46.10552
2.945	202.81994	2.013	4.39962	46.10552
3.1562	202.81994	2.013	4.39962	46.10552
3.13517	202.81994	2.013	4.39962	46.10552
2.68132	202.81994	2.013	4.39962	46.10552
3.10462	202.81994	2.013	4.39962	46.10552
3.0723	202.81994	2.013	4.39962	46.10552
3.11833	202.81994	2.013	4.39962	46.10552
3.11625	202.81994	2.013	4.39962	46.10552
3.08728	202.81994	2.013	4.39962	46.10552
3.0912	202.81994	2.013	4.39962	46.10552
3.22762	202.81994	2.013	4.39962	46.10552
2.89475	202.81994	2.013	4.39962	46.10552
2.3267	202.81994	2.013	4.39962	46.10552
2.37448	202.81994	2.013	4.39962	46.10552
3.15207	202.81994	2.013	4.39962	46.10552
2.7696	202.81994	2.013	4.39962	46.10552
2.9207	202.81994	2.013	4.39962	46.10552
2.9513	202.81994	2.013	4.39962	46.10552
2.3093	202.81994	2.013	4.39962	46.10552
3.12783	202.81994	2.013	4.39962	46.10552
3.10776	202.81994	2.013	4.39962	46.10552
3.15211	202.81994	2.013	4.39962	46.10552
2.32766	202.81994	2.013	4.39962	46.10552

3.05189	202.81994	2.013	4.39962	46.10552
---------	-----------	-------	---------	----------

## APPENDIX B

### **Abbreviations**

AASTHO- American Association of State Highway and Transportation Officials

AC-Alternative Current

ASTM-American Standard for Testing Materials

DC-Direct Current

APA-Asphalt Pavement Analyzer

CAD-Computer-Aided Design

LWT-Load Wheel Test

PLA-Polylactic Acid

PZT-Lead Zirconate Titanate

RMS-Root Mean Square

UL-Underwriters Laboratories

## APPENDIX C

Oscilloscope voltage (RMS) output display for PZT sensor no 22 embedded in circular shaped wafer box. The corresponding Excel file is given below (The total block size is 6006)



**Figure 70: Output display for PZT sensor no 22 embedded in circular shaped wafer box**

**Table 24: Data file for PZT sensor 22 embedded in circular shaped box**

<b>Header Size</b>	<b>15</b>
<b>Model Name</b>	<b>DL850</b>
<b>Comment</b>	
<b>BlockNumber</b>	<b>1</b>
<b>TraceName</b>	<b>CH4</b>
<b>BlockSize</b>	<b>6006</b>
<b>VUnit</b>	<b>V</b>
<b>SampleRate</b>	<b>100</b>

<b>HResolution</b>	<b>1.00E-02</b>
<b>HOffset</b>	<b>-6.01E+01</b>
<b>HUnit</b>	<b>s</b>
<b>DisplayPointNo.</b>	<b>1</b>
<b>PhaseShift</b>	<b>1</b>
<b>Date</b>	<b>2/24/2018</b>
<b>Time</b>	<b>33:28.3</b>
1	3.30E+00
2	3.30E+00
3	3.29E+00
4	3.28E+00
5	3.28E+00
6	3.28E+00
7	3.28E+00
8	3.26E+00
9	3.27E+00
10	3.27E+00
11	3.26E+00
12	3.25E+00
13	3.26E+00
14	3.26E+00
15	3.26E+00
16	3.26E+00
17	3.25E+00
18	3.25E+00
19	3.25E+00
20	3.26E+00
21	3.25E+00
22	3.24E+00
23	3.25E+00
24	3.25E+00
25	3.27E+00
26	3.28E+00
27	3.28E+00
28	3.30E+00
29	3.31E+00
30	3.31E+00
31	3.33E+00
32	3.33E+00

33	3.33E+00
34	3.33E+00
35	3.36E+00
36	3.38E+00
37	3.39E+00
38	3.40E+00
39	3.42E+00
40	3.43E+00
41	3.44E+00
42	3.44E+00
43	3.42E+00
44	3.43E+00
45	3.43E+00
46	3.42E+00
47	3.43E+00
48	3.45E+00
49	3.45E+00
50	3.46E+00
51	3.47E+00
52	3.46E+00
53	3.46E+00
54	3.46E+00
55	3.45E+00
56	3.47E+00
57	3.46E+00
58	3.47E+00
59	3.46E+00
60	3.47E+00
61	3.46E+00
62	3.46E+00
63	3.46E+00
64	3.47E+00
65	3.46E+00
66	3.47E+00
67	3.47E+00
68	3.47E+00
69	3.46E+00
70	3.47E+00
71	3.46E+00

72	3.46E+00
73	3.46E+00
74	3.46E+00
75	3.46E+00
76	3.45E+00
77	3.46E+00
78	3.46E+00
79	3.45E+00
80	3.44E+00
81	3.45E+00
82	3.44E+00
83	3.44E+00
84	3.44E+00
85	3.44E+00
86	3.44E+00
87	3.44E+00
88	3.42E+00
89	3.42E+00
90	3.43E+00
91	3.42E+00
92	3.42E+00
93	3.41E+00
94	3.41E+00
95	3.41E+00
96	3.40E+00
97	3.40E+00
98	3.40E+00
99	3.38E+00
100	3.39E+00
101	3.39E+00
102	3.38E+00
103	3.37E+00
104	3.39E+00
105	3.37E+00
106	3.37E+00
107	3.38E+00
108	3.38E+00
109	3.38E+00
110	3.39E+00

111	3.39E+00
112	3.39E+00
113	3.39E+00
114	3.39E+00
115	3.41E+00
116	3.42E+00
117	3.43E+00
118	3.44E+00
119	3.45E+00
120	3.45E+00
121	3.44E+00
122	3.44E+00
123	3.44E+00
124	3.43E+00
125	3.44E+00
126	3.44E+00
127	3.43E+00
128	3.43E+00
129	3.45E+00
130	3.44E+00
131	3.44E+00
132	3.45E+00
133	3.46E+00
134	3.46E+00
135	3.46E+00
136	3.45E+00
137	3.46E+00
138	3.46E+00
139	3.47E+00
140	3.46E+00
141	3.47E+00
142	3.48E+00
143	3.47E+00
144	3.48E+00
145	3.48E+00
146	3.48E+00
147	3.49E+00
148	3.47E+00
149	3.48E+00



150	3.48E+00
151	3.48E+00
152	3.49E+00
153	3.48E+00
154	3.48E+00
155	3.49E+00
156	3.49E+00
157	3.50E+00
158	3.48E+00
159	3.47E+00
160	3.50E+00
161	3.51E+00
162	3.51E+00
163	3.50E+00
164	3.50E+00
165	3.49E+00
166	3.50E+00
167	3.50E+00
168	3.50E+00
169	3.49E+00
170	3.48E+00
171	3.49E+00
172	3.50E+00
173	3.48E+00
174	3.48E+00
175	3.48E+00
176	3.47E+00
177	3.47E+00
178	3.47E+00
179	3.46E+00
180	3.47E+00
181	3.47E+00
182	3.46E+00
183	3.45E+00
184	3.45E+00
185	3.45E+00
186	3.45E+00
187	3.45E+00
188	3.44E+00

189	3.43E+00
190	3.44E+00
191	3.44E+00
192	3.44E+00
193	3.42E+00
194	3.42E+00
195	3.42E+00
196	3.43E+00
197	3.41E+00
198	3.41E+00
199	3.41E+00
200	3.41E+00
201	3.40E+00
202	3.41E+00
203	3.40E+00
204	3.39E+00
205	3.39E+00
206	3.39E+00
207	3.38E+00
208	3.37E+00
209	3.38E+00
210	3.36E+00
211	3.38E+00
212	3.37E+00
213	3.36E+00
214	3.37E+00
215	3.36E+00
216	3.36E+00
217	3.37E+00
218	3.35E+00
219	3.35E+00
220	3.35E+00
221	3.34E+00
222	3.34E+00
223	3.34E+00
224	3.34E+00
225	3.33E+00
226	3.34E+00
227	3.33E+00

228	3.33E+00
229	3.34E+00
230	3.33E+00
231	3.34E+00
232	3.33E+00
233	3.35E+00
234	3.36E+00
235	3.37E+00
236	3.37E+00
237	3.37E+00
238	3.39E+00
239	3.39E+00
240	3.39E+00
241	3.41E+00
242	3.42E+00
243	3.43E+00
244	3.44E+00
245	3.47E+00
246	3.48E+00
247	3.50E+00
248	3.49E+00
249	3.51E+00
250	3.51E+00
251	3.50E+00
252	3.51E+00
253	3.49E+00
254	3.50E+00
255	3.49E+00
256	3.52E+00
257	3.53E+00
258	3.55E+00
259	3.53E+00
260	3.52E+00
261	3.54E+00
262	3.53E+00
263	3.53E+00
264	3.55E+00
265	3.54E+00
266	3.53E+00

267	3.54E+00
268	3.54E+00
269	3.53E+00
Continuous	
Continuous	
Continuous	
Continuous	
Continuous	
Continuous	
Continuous	
Continuous	
6001	3.53E+00
6001	3.54E+00
6002	3.54E+00
6003	3.54E+00
6004	3.54E+00
6005	3.53E+00
6006	3.53E+00

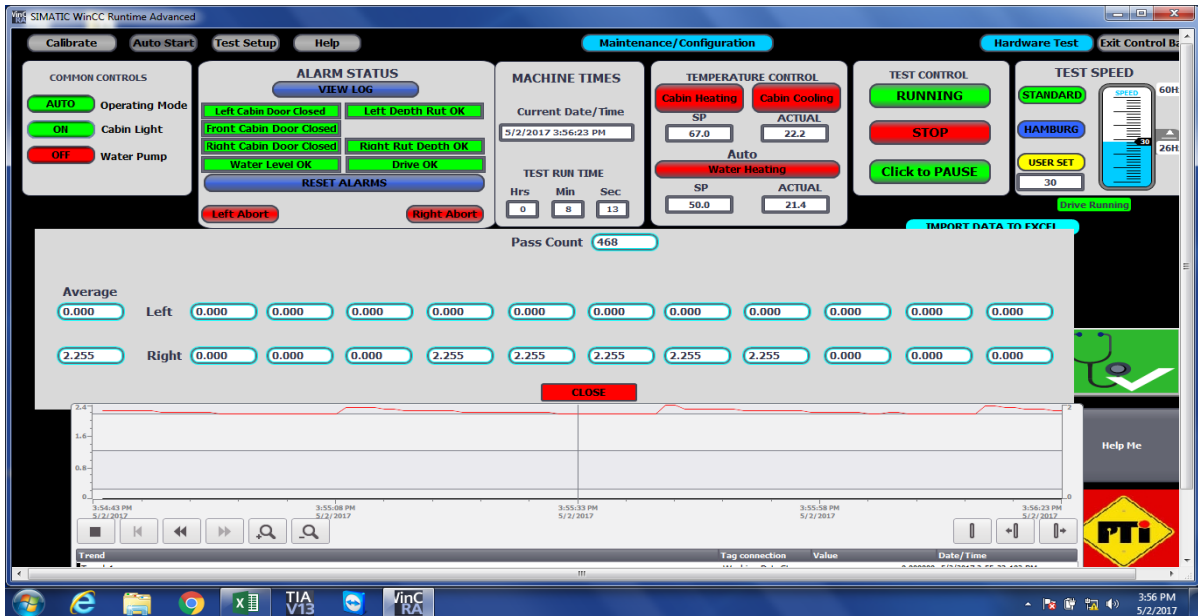


Figure 71: Control interface of APA-Jr software.

## APPENDIX D

The studentized range statistic (q)\*

\*The critical values for q corresponding to  $\alpha = .05$  (top) and  $\alpha = .01$  (bottom)

df for Error Term	k= Number of Treatments								
	2	3	4	5	6	7	8	9	10
5	3.64	4.60	5.22	5.67	6.03	6.33	6.58	6.80	6.99
	5.70	6.98	7.80	8.42	8.91	9.32	9.67	9.97	10.24
6	3.46	4.34	4.90	5.30	5.63	5.90	6.12	6.32	6.49
	5.24	6.33	7.03	7.56	7.97	8.32	8.61	8.87	9.10
7	3.34	4.16	4.68	5.06	5.36	5.61	5.82	6.00	6.16
	4.95	5.92	6.54	7.01	7.37	7.68	7.94	8.17	8.37
8	3.26	4.04	4.53	4.89	5.17	5.40	5.60	5.77	5.92
	4.75	5.64	6.20	6.62	6.96	7.24	7.47	7.68	7.86
9	3.20	3.95	4.41	4.76	5.02	5.24	5.43	5.59	5.74
	4.60	5.43	5.96	6.35	6.66	6.91	7.13	7.33	7.49
10	3.15	3.88	4.33	4.65	4.91	5.12	5.30	5.46	5.60
	4.48	5.27	5.77	6.14	6.43	6.67	6.87	7.05	7.21
11	3.11	3.82	4.26	4.57	4.82	5.03	5.20	5.35	5.49
	4.39	5.15	5.62	5.97	6.25	6.48	6.67	6.84	6.99
12	3.08	3.77	4.20	4.51	4.75	4.95	5.12	5.27	5.39
	4.32	5.05	5.50	5.84	6.10	6.32	6.51	6.67	6.81
13	3.06	3.73	4.15	4.45	4.69	4.88	5.05	5.19	5.32
	4.26	4.96	5.40	5.73	5.98	6.19	6.37	6.53	6.67
14	3.03	3.70	4.11	4.41	4.64	4.83	4.99	5.13	5.25
	4.21	4.89	5.32	5.63	5.88	6.08	6.26	6.41	6.54
15	3.01	3.67	4.08	4.37	4.59	4.78	4.94	5.08	5.20
	4.17	4.84	5.25	5.56	5.80	5.99	6.16	6.31	6.44
16	3.00	3.65	4.05	4.33	4.56	4.74	4.90	5.03	5.15
	4.13	4.79	5.19	5.49	5.72	5.92	6.08	6.22	6.35
17	2.98	3.63	4.02	4.30	4.52	4.70	4.86	4.99	5.11
	4.10	4.74	5.14	5.43	5.66	5.85	6.01	6.15	6.27

Source: <http://www2.stat.duke.edu/courses/Spring98/sta110c/qtable.html>

The studentized range statistic (q)\* (continued)

\*The critical values for q corresponding to  $\alpha = .05$  (top) and  $\alpha = .01$  (bottom)

17	2.98 4.10	3.63 4.74	4.02 5.14	4.30 5.43	4.52 5.66	4.70 5.85	4.86 6.01	4.99 6.15	5.11 6.27
18	2.97 4.07	3.61 4.70	4.00 5.09	4.28 5.38	4.49 5.60	4.67 5.79	4.82 5.94	4.96 6.08	5.07 6.20
19	2.96 4.05	3.59 4.67	3.98 5.05	4.25 5.33	4.47 5.55	4.65 5.73	4.79 5.89	4.92 6.02	5.04 6.14
20	2.95 4.02	3.58 4.64	3.96 5.02	4.23 5.29	4.45 5.51	4.62 5.69	4.77 5.84	4.90 5.97	5.01 6.09
24	2.92 3.96	3.53 4.55	3.90 4.91	4.17 5.17	4.37 5.37	4.54 5.54	4.68 5.69	4.81 5.81	4.92 5.92
30	2.89 3.89	3.49 4.45	3.85 4.80	4.10 5.05	4.30 5.24	4.46 5.40	4.60 5.54	4.72 5.65	4.82 5.76
40	2.86 3.82	3.44 4.37	3.79 4.70	4.04 4.93	4.23 5.11	4.39 5.26	4.52 5.39	4.63 5.50	4.73 5.60
60	2.83 3.76	3.40 4.28	3.74 4.59	3.98 4.82	4.16 4.99	4.31 5.13	4.44 5.25	4.55 5.36	4.65 5.45
120	2.80 3.70	3.36 4.20	3.68 4.50	3.92 4.71	4.10 4.87	4.24 5.01	4.36 5.12	4.47 5.21	4.56 5.30
infinity	2.77 3.64	3.31 4.12	3.63 4.40	3.86 4.60	4.03 4.76	4.17 4.88	4.29 4.99	4.39 5.08	4.47 5.16

Source: <http://www2.stat.duke.edu/courses/Spring98/sta110c/qtable.html>

**Table of critical values for the F distribution (for use with ANOVA):**

**How to use this table:**

There are two tables here. The first one gives critical values of F at the  $p = 0.05$  level of significance.

The second table gives critical values of F at the  $p = 0.01$  level of significance.

1. Obtain your F-ratio. This has (x,y) degrees of freedom associated with it.

2. Go along x columns, and down y rows. The point of intersection is your critical F-ratio.

3. If your obtained value of F is equal to or larger than this critical F-value, then your result is significant at that level of probability.

An example: I obtain an F ratio of 3.96 with (2, 24) degrees of freedom.

I go along 2 columns and down 24 rows. The critical value of F is 3.40. My obtained F-ratio

is larger than this, and so I conclude that my obtained F-ratio is likely to occur by chance with a  $p < .05$ .

**Critical values of F for the 0.05 significance level:**

	1	2	3	4	5	6	7	8	9	10
1	161.45	199.50	215.71	224.58	230.16	233.99	236.77	238.88	240.54	241.88
2	18.51	19.00	19.16	19.25	19.30	19.33	19.35	19.37	19.39	19.40
3	10.13	9.55	9.28	9.12	9.01	8.94	8.89	8.85	8.81	8.79
4	7.71	6.94	6.59	6.39	6.26	6.16	6.09	6.04	6.00	5.96
5	6.61	5.79	5.41	5.19	5.05	4.95	4.88	4.82	4.77	4.74
6	5.99	5.14	4.76	4.53	4.39	4.28	4.21	4.15	4.10	4.06
7	5.59	4.74	4.35	4.12	3.97	3.87	3.79	3.73	3.68	3.64
8	5.32	4.46	4.07	3.84	3.69	3.58	3.50	3.44	3.39	3.35
9	5.12	4.26	3.86	3.63	3.48	3.37	3.29	3.23	3.18	3.14
10	4.97	4.10	3.71	3.48	3.33	3.22	3.14	3.07	3.02	2.98
11	4.84	3.98	3.59	3.36	3.20	3.10	3.01	2.95	2.90	2.85
12	4.75	3.89	3.49	3.26	3.11	3.00	2.91	2.85	2.80	2.75
13	4.67	3.81	3.41	3.18	3.03	2.92	2.83	2.77	2.71	2.67
14	4.60	3.74	3.34	3.11	2.96	2.85	2.76	2.70	2.65	2.60
15	4.54	3.68	3.29	3.06	2.90	2.79	2.71	2.64	2.59	2.54
16	4.49	3.63	3.24	3.01	2.85	2.74	2.66	2.59	2.54	2.49
17	4.45	3.59	3.20	2.97	2.81	2.70	2.61	2.55	2.49	2.45
18	4.41	3.56	3.16	2.93	2.77	2.66	2.58	2.51	2.46	2.41
19	4.38	3.52	3.13	2.90	2.74	2.63	2.54	2.48	2.42	2.38
20	4.35	3.49	3.10	2.87	2.71	2.60	2.51	2.45	2.39	2.35
21	4.33	3.47	3.07	2.84	2.69	2.57	2.49	2.42	2.37	2.32
22	4.30	3.44	3.05	2.82	2.66	2.55	2.46	2.40	2.34	2.30
23	4.28	3.42	3.03	2.80	2.64	2.53	2.44	2.38	2.32	2.28
24	4.26	3.40	3.01	2.78	2.62	2.51	2.42	2.36	2.30	2.26
25	4.24	3.39	2.99	2.76	2.60	2.49	2.41	2.34	2.28	2.24
26	4.23	3.37	2.98	2.74	2.59	2.47	2.39	2.32	2.27	2.22
27	4.21	3.35	2.96	2.73	2.57	2.46	2.37	2.31	2.25	2.20
28	4.20	3.34	2.95	2.71	2.56	2.45	2.36	2.29	2.24	2.19
29	4.18	3.33	2.93	2.70	2.55	2.43	2.35	2.28	2.22	2.18
30	4.17	3.32	2.92	2.69	2.53	2.42	2.33	2.27	2.21	2.17
31	4.16	3.31	2.91	2.68	2.52	2.41	2.32	2.26	2.20	2.15
32	4.15	3.30	2.90	2.67	2.51	2.40	2.31	2.24	2.19	2.14
33	4.14	3.29	2.89	2.66	2.50	2.39	2.30	2.24	2.18	2.13
34	4.13	3.28	2.88	2.65	2.49	2.38	2.29	2.23	2.17	2.12
35	4.12	3.27	2.87	2.64	2.49	2.37	2.29	2.22	2.16	2.11

Source: <http://users.sussex.ac.uk/~grahamh/RM1web/F-ratio%20table%202005.pdf>



36	4.11	3.26	2.87	2.63	2.48	2.36	2.28	2.21	2.15	2.11
37	4.11	3.25	2.86	2.63	2.47	2.36	2.27	2.20	2.15	2.10
38	4.10	3.25	2.85	2.62	2.46	2.35	2.26	2.19	2.14	2.09
39	4.09	3.24	2.85	2.61	2.46	2.34	2.26	2.19	2.13	2.08
40	4.09	3.23	2.84	2.61	2.45	2.34	2.25	2.18	2.12	2.08
41	4.08	3.23	2.83	2.60	2.44	2.33	2.24	2.17	2.12	2.07
42	4.07	3.22	2.83	2.59	2.44	2.32	2.24	2.17	2.11	2.07
43	4.07	3.21	2.82	2.59	2.43	2.32	2.23	2.16	2.11	2.06
44	4.06	3.21	2.82	2.58	2.43	2.31	2.23	2.16	2.10	2.05
45	4.06	3.20	2.81	2.58	2.42	2.31	2.22	2.15	2.10	2.05
46	4.05	3.20	2.81	2.57	2.42	2.30	2.22	2.15	2.09	2.04
47	4.05	3.20	2.80	2.57	2.41	2.30	2.21	2.14	2.09	2.04
48	4.04	3.19	2.80	2.57	2.41	2.30	2.21	2.14	2.08	2.04
49	4.04	3.19	2.79	2.56	2.40	2.29	2.20	2.13	2.08	2.03
50	4.03	3.18	2.79	2.56	2.40	2.29	2.20	2.13	2.07	2.03
51	4.03	3.18	2.79	2.55	2.40	2.28	2.20	2.13	2.07	2.02
52	4.03	3.18	2.78	2.55	2.39	2.28	2.19	2.12	2.07	2.02
53	4.02	3.17	2.78	2.55	2.39	2.28	2.19	2.12	2.06	2.02
54	4.02	3.17	2.78	2.54	2.39	2.27	2.19	2.12	2.06	2.01
55	4.02	3.17	2.77	2.54	2.38	2.27	2.18	2.11	2.06	2.01
56	4.01	3.16	2.77	2.54	2.38	2.27	2.18	2.11	2.05	2.01
57	4.01	3.16	2.77	2.53	2.38	2.26	2.18	2.11	2.05	2.00
58	4.01	3.16	2.76	2.53	2.37	2.26	2.17	2.10	2.05	2.00
59	4.00	3.15	2.76	2.53	2.37	2.26	2.17	2.10	2.04	2.00
60	4.00	3.15	2.76	2.53	2.37	2.25	2.17	2.10	2.04	1.99
61	4.00	3.15	2.76	2.52	2.37	2.25	2.16	2.09	2.04	1.99
62	4.00	3.15	2.75	2.52	2.36	2.25	2.16	2.09	2.04	1.99
63	3.99	3.14	2.75	2.52	2.36	2.25	2.16	2.09	2.03	1.99
64	3.99	3.14	2.75	2.52	2.36	2.24	2.16	2.09	2.03	1.98
65	3.99	3.14	2.75	2.51	2.36	2.24	2.15	2.08	2.03	1.98
66	3.99	3.14	2.74	2.51	2.35	2.24	2.15	2.08	2.03	1.98
67	3.98	3.13	2.74	2.51	2.35	2.24	2.15	2.08	2.02	1.98
68	3.98	3.13	2.74	2.51	2.35	2.24	2.15	2.08	2.02	1.97
69	3.98	3.13	2.74	2.51	2.35	2.23	2.15	2.08	2.02	1.97
70	3.98	3.13	2.74	2.50	2.35	2.23	2.14	2.07	2.02	1.97
71	3.98	3.13	2.73	2.50	2.34	2.23	2.14	2.07	2.02	1.97
72	3.97	3.12	2.73	2.50	2.34	2.23	2.14	2.07	2.01	1.97
73	3.97	3.12	2.73	2.50	2.34	2.23	2.14	2.07	2.01	1.96
74	3.97	3.12	2.73	2.50	2.34	2.22	2.14	2.07	2.01	1.96
75	3.97	3.12	2.73	2.49	2.34	2.22	2.13	2.06	2.01	1.96
76	3.97	3.12	2.73	2.49	2.34	2.22	2.13	2.06	2.01	1.96
77	3.97	3.12	2.72	2.49	2.33	2.22	2.13	2.06	2.00	1.96
78	3.96	3.11	2.72	2.49	2.33	2.22	2.13	2.06	2.00	1.95
79	3.96	3.11	2.72	2.49	2.33	2.22	2.13	2.06	2.00	1.95
80	3.96	3.11	2.72	2.49	2.33	2.21	2.13	2.06	2.00	1.95
81	3.96	3.11	2.72	2.48	2.33	2.21	2.13	2.06	2.00	1.95
82	3.96	3.11	2.72	2.48	2.33	2.21	2.12	2.05	2.00	1.95
83	3.96	3.11	2.72	2.48	2.32	2.21	2.12	2.05	2.00	1.95
84	3.96	3.11	2.71	2.48	2.32	2.21	2.12	2.05	1.99	1.95
85	3.95	3.10	2.71	2.48	2.32	2.21	2.12	2.05	1.99	1.94

Source: <http://users.sussex.ac.uk/~grahamh/RM1web/F-ratio%20table%202005.pdf>

86	3.95	3.10	2.71	2.48	2.32	2.21	2.12	2.05	1.99	1.94
87	3.95	3.10	2.71	2.48	2.32	2.21	2.12	2.05	1.99	1.94
88	3.95	3.10	2.71	2.48	2.32	2.20	2.12	2.05	1.99	1.94
89	3.95	3.10	2.71	2.47	2.32	2.20	2.11	2.04	1.99	1.94
90	3.95	3.10	2.71	2.47	2.32	2.20	2.11	2.04	1.99	1.94
91	3.95	3.10	2.71	2.47	2.32	2.20	2.11	2.04	1.98	1.94
92	3.95	3.10	2.70	2.47	2.31	2.20	2.11	2.04	1.98	1.94
93	3.94	3.09	2.70	2.47	2.31	2.20	2.11	2.04	1.98	1.93
94	3.94	3.09	2.70	2.47	2.31	2.20	2.11	2.04	1.98	1.93
95	3.94	3.09	2.70	2.47	2.31	2.20	2.11	2.04	1.98	1.93
96	3.94	3.09	2.70	2.47	2.31	2.20	2.11	2.04	1.98	1.93
97	3.94	3.09	2.70	2.47	2.31	2.19	2.11	2.04	1.98	1.93
98	3.94	3.09	2.70	2.47	2.31	2.19	2.10	2.03	1.98	1.93
99	3.94	3.09	2.70	2.46	2.31	2.19	2.10	2.03	1.98	1.93
100	3.94	3.09	2.70	2.46	2.31	2.19	2.10	2.03	1.98	1.93

**Critical values of F for the 0.01 significance level:**

	1	2	3	4	5	6	7	8	9	10
1	4052.19	4999.52	5403.34	5624.62	5763.65	5858.97	5928.33	5981.10	6022.50	6055.85
2	98.50	99.00	99.17	99.25	99.30	99.33	99.36	99.37	99.39	99.40
3	34.12	30.82	29.46	28.71	28.24	27.91	27.67	27.49	27.35	27.23
4	21.20	18.00	16.69	15.98	15.52	15.21	14.98	14.80	14.66	14.55
5	16.26	13.27	12.06	11.39	10.97	10.67	10.46	10.29	10.16	10.05
6	13.75	10.93	9.78	9.15	8.75	8.47	8.26	8.10	7.98	7.87
7	12.25	9.55	8.45	7.85	7.46	7.19	6.99	6.84	6.72	6.62
8	11.26	8.65	7.59	7.01	6.63	6.37	6.18	6.03	5.91	5.81
9	10.56	8.02	6.99	6.42	6.06	5.80	5.61	5.47	5.35	5.26
10	10.04	7.56	6.55	5.99	5.64	5.39	5.20	5.06	4.94	4.85
11	9.65	7.21	6.22	5.67	5.32	5.07	4.89	4.74	4.63	4.54
12	9.33	6.93	5.95	5.41	5.06	4.82	4.64	4.50	4.39	4.30
13	9.07	6.70	5.74	5.21	4.86	4.62	4.44	4.30	4.19	4.10
14	8.86	6.52	5.56	5.04	4.70	4.46	4.28	4.14	4.03	3.94
15	8.68	6.36	5.42	4.89	4.56	4.32	4.14	4.00	3.90	3.81
16	8.53	6.23	5.29	4.77	4.44	4.20	4.03	3.89	3.78	3.69
17	8.40	6.11	5.19	4.67	4.34	4.10	3.93	3.79	3.68	3.59
18	8.29	6.01	5.09	4.58	4.25	4.02	3.84	3.71	3.60	3.51
19	8.19	5.93	5.01	4.50	4.17	3.94	3.77	3.63	3.52	3.43
20	8.10	5.85	4.94	4.43	4.10	3.87	3.70	3.56	3.46	3.37
21	8.02	5.78	4.87	4.37	4.04	3.81	3.64	3.51	3.40	3.31
22	7.95	5.72	4.82	4.31	3.99	3.76	3.59	3.45	3.35	3.26
23	7.88	5.66	4.77	4.26	3.94	3.71	3.54	3.41	3.30	3.21
24	7.82	5.61	4.72	4.22	3.90	3.67	3.50	3.36	3.26	3.17
25	7.77	5.57	4.68	4.18	3.86	3.63	3.46	3.32	3.22	3.13
26	7.72	5.53	4.64	4.14	3.82	3.59	3.42	3.29	3.18	3.09
27	7.68	5.49	4.60	4.11	3.79	3.56	3.39	3.26	3.15	3.06
28	7.64	5.45	4.57	4.07	3.75	3.53	3.36	3.23	3.12	3.03
29	7.60	5.42	4.54	4.05	3.73	3.50	3.33	3.20	3.09	3.01
30	7.56	5.39	4.51	4.02	3.70	3.47	3.31	3.17	3.07	2.98
31	7.53	5.36	4.48	3.99	3.68	3.45	3.28	3.15	3.04	2.96
32	7.50	5.34	4.46	3.97	3.65	3.43	3.26	3.13	3.02	2.93

Source: <http://users.sussex.ac.uk/~grahamh/RM1web/F-ratio%20table%202005.pdf>

33	7.47	5.31	4.44	3.95	3.63	3.41	3.24	3.11	3.00	2.91
34	7.44	5.29	4.42	3.93	3.61	3.39	3.22	3.09	2.98	2.89
35	7.42	5.27	4.40	3.91	3.59	3.37	3.20	3.07	2.96	2.88
36	7.40	5.25	4.38	3.89	3.57	3.35	3.18	3.05	2.95	2.86
37	7.37	5.23	4.36	3.87	3.56	3.33	3.17	3.04	2.93	2.84
38	7.35	5.21	4.34	3.86	3.54	3.32	3.15	3.02	2.92	2.83
39	7.33	5.19	4.33	3.84	3.53	3.31	3.14	3.01	2.90	2.81
40	7.31	5.18	4.31	3.83	3.51	3.29	3.12	2.99	2.89	2.80
41	7.30	5.16	4.30	3.82	3.50	3.28	3.11	2.98	2.88	2.79
42	7.28	5.15	4.29	3.80	3.49	3.27	3.10	2.97	2.86	2.78
43	7.26	5.14	4.27	3.79	3.48	3.25	3.09	2.96	2.85	2.76
44	7.25	5.12	4.26	3.78	3.47	3.24	3.08	2.95	2.84	2.75
45	7.23	5.11	4.25	3.77	3.45	3.23	3.07	2.94	2.83	2.74
46	7.22	5.10	4.24	3.76	3.44	3.22	3.06	2.93	2.82	2.73
47	7.21	5.09	4.23	3.75	3.43	3.21	3.05	2.92	2.81	2.72
48	7.19	5.08	4.22	3.74	3.43	3.20	3.04	2.91	2.80	2.72
49	7.18	5.07	4.21	3.73	3.42	3.20	3.03	2.90	2.79	2.71
50	7.17	5.06	4.20	3.72	3.41	3.19	3.02	2.89	2.79	2.70
51	7.16	5.05	4.19	3.71	3.40	3.18	3.01	2.88	2.78	2.69
52	7.15	5.04	4.18	3.70	3.39	3.17	3.01	2.87	2.77	2.68
53	7.14	5.03	4.17	3.70	3.38	3.16	3.00	2.87	2.76	2.68
54	7.13	5.02	4.17	3.69	3.38	3.16	2.99	2.86	2.76	2.67
55	7.12	5.01	4.16	3.68	3.37	3.15	2.98	2.85	2.75	2.66
56	7.11	5.01	4.15	3.67	3.36	3.14	2.98	2.85	2.74	2.66
57	7.10	5.00	4.15	3.67	3.36	3.14	2.97	2.84	2.74	2.65
58	7.09	4.99	4.14	3.66	3.35	3.13	2.97	2.84	2.73	2.64
59	7.09	4.98	4.13	3.66	3.35	3.12	2.96	2.83	2.72	2.64
60	7.08	4.98	4.13	3.65	3.34	3.12	2.95	2.82	2.72	2.63
61	7.07	4.97	4.12	3.64	3.33	3.11	2.95	2.82	2.71	2.63
62	7.06	4.97	4.11	3.64	3.33	3.11	2.94	2.81	2.71	2.62
63	7.06	4.96	4.11	3.63	3.32	3.10	2.94	2.81	2.70	2.62
64	7.05	4.95	4.10	3.63	3.32	3.10	2.93	2.80	2.70	2.61
65	7.04	4.95	4.10	3.62	3.31	3.09	2.93	2.80	2.69	2.61
66	7.04	4.94	4.09	3.62	3.31	3.09	2.92	2.79	2.69	2.60
67	7.03	4.94	4.09	3.61	3.30	3.08	2.92	2.79	2.68	2.60
68	7.02	4.93	4.08	3.61	3.30	3.08	2.91	2.79	2.68	2.59
69	7.02	4.93	4.08	3.60	3.30	3.08	2.91	2.78	2.68	2.59
70	7.01	4.92	4.07	3.60	3.29	3.07	2.91	2.78	2.67	2.59
71	7.01	4.92	4.07	3.60	3.29	3.07	2.90	2.77	2.67	2.58
72	7.00	4.91	4.07	3.59	3.28	3.06	2.90	2.77	2.66	2.58
73	7.00	4.91	4.06	3.59	3.28	3.06	2.90	2.77	2.66	2.57
74	6.99	4.90	4.06	3.58	3.28	3.06	2.89	2.76	2.66	2.57
75	6.99	4.90	4.05	3.58	3.27	3.05	2.89	2.76	2.65	2.57
76	6.98	4.90	4.05	3.58	3.27	3.05	2.88	2.76	2.65	2.56
77	6.98	4.89	4.05	3.57	3.27	3.05	2.88	2.75	2.65	2.56
78	6.97	4.89	4.04	3.57	3.26	3.04	2.88	2.75	2.64	2.56
79	6.97	4.88	4.04	3.57	3.26	3.04	2.87	2.75	2.64	2.55
80	6.96	4.88	4.04	3.56	3.26	3.04	2.87	2.74	2.64	2.55
81	6.96	4.88	4.03	3.56	3.25	3.03	2.87	2.74	2.63	2.55
82	6.95	4.87	4.03	3.56	3.25	3.03	2.87	2.74	2.63	2.55

Source: <http://users.sussex.ac.uk/~grahamh/RM1web/F-ratio%20table%202005.pdf>

83	6.95	4.87	4.03	3.55	3.25	3.03	2.86	2.73	2.63	2.54
84	6.95	4.87	4.02	3.55	3.24	3.03	2.86	2.73	2.63	2.54
85	6.94	4.86	4.02	3.55	3.24	3.02	2.86	2.73	2.62	2.54
86	6.94	4.86	4.02	3.55	3.24	3.02	2.85	2.73	2.62	2.53
87	6.94	4.86	4.02	3.54	3.24	3.02	2.85	2.72	2.62	2.53
88	6.93	4.86	4.01	3.54	3.23	3.01	2.85	2.72	2.62	2.53
89	6.93	4.85	4.01	3.54	3.23	3.01	2.85	2.72	2.61	2.53
90	6.93	4.85	4.01	3.54	3.23	3.01	2.85	2.72	2.61	2.52
91	6.92	4.85	4.00	3.53	3.23	3.01	2.84	2.71	2.61	2.52
92	6.92	4.84	4.00	3.53	3.22	3.00	2.84	2.71	2.61	2.52
93	6.92	4.84	4.00	3.53	3.22	3.00	2.84	2.71	2.60	2.52
94	6.91	4.84	4.00	3.53	3.22	3.00	2.84	2.71	2.60	2.52
95	6.91	4.84	4.00	3.52	3.22	3.00	2.83	2.70	2.60	2.51
96	6.91	4.83	3.99	3.52	3.21	3.00	2.83	2.70	2.60	2.51
97	6.90	4.83	3.99	3.52	3.21	2.99	2.83	2.70	2.60	2.51
98	6.90	4.83	3.99	3.52	3.21	2.99	2.83	2.70	2.59	2.51
99	6.90	4.83	3.99	3.52	3.21	2.99	2.83	2.70	2.59	2.51
100	6.90	4.82	3.98	3.51	3.21	2.99	2.82	2.69	2.59	2.50

Source: <http://users.sussex.ac.uk/~grahamh/RM1web/F-ratio%20table%202005.pdf>